

Wide low and VLM binary systems using VO tools

M. C. Gálvez-Ortiz,^{1,2*} E. Solano,^{3,4} N. Lodieu,^{5,6} and M. Aberasturi⁷

¹ *Centro de Astrobiología (CSIC-INTA), Ctra. Ajalvir km 4, E-28850 Torrejón de Ardoz, Madrid, Spain.*

² *Centre for Astrophysics Research, Science and Technology Research Institute, University of Hertfordshire, Hatfield AL10 9AB, UK.*

³ *Centro de Astrobiología (INTA-CSIC), Departamento de Astrofísica, P.O. Box 78, E-28691 Villanueva de la Cañada, Madrid, Spain.*

⁴ *Spanish Virtual Observatory.*

⁵ *Instituto de Astrofísica de Canarias (IAC), Calle Vía Láctea s/n, E-38200 La Laguna, Tenerife, Spain.*

⁶ *Departamento de Astrofísica, Universidad de La Laguna (ULL), E-38205 La Laguna, Tenerife, Spain IAC.*

⁷ *ESA-ESAC, SOC. P.O. Box 78, E-28691 Villanueva de la Cañada, Madrid, Spain.*

Accepted 1988 December 15. Received 1988 December 14; in original form 1988 October 11

ABSTRACT

The frequency of multiple systems and their properties are key constraints of stellar formation and evolution. Formation mechanisms of very low-mass (VLM) objects are still under considerable debate and an accurate assessment of their multiplicity and orbital properties are essential for constraining current theoretical models.

Taking advantage of the Virtual Observatory capabilities, we looked for comoving low and VLM binary (or multiple) systems using the Large Area Survey of the UKIDSS LAS DR10, SDSS DR9, and the 2MASS Catalogues. Other catalogues (*WISE*, *GLIMPSE*, *SuperCosmos* ...) were used to derive the physical parameters of the systems.

We report the identification of 36 low and VLM (\sim M0-L0 spectral types) candidates to binary/multiple system (separations between 200 and 92000 AU), whose physical association is confirmed through common proper motion, distance and low probability of chance alignment. This new system list notably increases the previous sampling in their mass-separation parameter space (\sim 100). We have also found 50 low-mass objects that we can classify as \sim L0-T2 according to their photometric information. Only one of these objects presents a common proper motion high-mass companion.

Although we could not constrain the age of the majority of the candidates, probably most of them are still bound except four that may be under disruption processes. We suggest that our sample could be divided in two populations: one tightly bound wide VLM systems that are expected to last more than 10 Gyr, and other formed by weak bound wide VLM systems that will dissipate within a few Gyrs.

Key words: Astronomical data bases: miscellaneous – Virtual Observatory tools – binaries: general – brown dwarfs

1 INTRODUCTION

Binary and multiple stars have long provided an empirical effective method of testing stellar formation and evolution theories.

Our understanding of formation and evolution processes in very low-mass stellar (VLM) and substellar objects is still not clear. Here we define VLM stars as fully convective stars with masses under $0.3 M_{\odot}$ (which typically corresponds to spectral types M3-M4) and above the substellar limit ($0.075 M_{\odot}$; Martín 2000). Ultracool dwarfs (UCDs) refers to ob-

jects with spectral type of M7 or later corresponding to $T_{eff} \leq 2500$ K, the spectra of which are dominated by molecular bands and dust (e.g. Knapp et al. 2004; Burgasser, Burrows & Kirkpatrick 2006).

Whether these cool objects form in a similar manner to higher mass stars or require additional or different processes is currently under debate (e.g., Burgasser et al. 2007; Luhman et al. 2007; Whitworth et al. 2007; Luhman 2012; Chabrier et al. 2014). Since multiplicity properties such as binary fraction, period and mass-ratio distribution or separation, provide important constraints on star formation and dynamical evolution (Burgasser et al. 2007; Goodwin & Whitworth 2007), it is of considerable interest to deter-

* E-mail:mcz@cab.inta-csic.es

mine whether the properties of VLM binaries differ from those of more massive stars (see, for instance, Duquennoy & Mayor 1991 and Fischer & Marcy 1992).

Many works have estimated binary fraction and the mass-ratio distribution. Burgasser et al. (2007) presented an extensive review on the multiplicity of VLM objects, reporting important differences between them and the more massive stars. In particular, VLM objects show a lower multiplicity ratio, 20-25% (Kraus & Hillenbrand 2012), compared to $\approx 80\%$ for B stars (Kouwenhoven et al. 2005), $\approx 65\%$ for G stars (Duquennoy & Mayor 1991) and $\approx 40\%$ for M2-M5 dwarfs (Fischer & Marcy 1992), and the mass-ratio distribution strongly peaks at unity whereas it is more evenly distributed for more massive stars. Also, the separation between components is significantly smaller for VLM objects. Typical separation is ~ 4 AU (e.g. Close et al. 2003; Burgasser et al. 2007; Kraus & Hillenbrand 2012), from statistical samples with separation over 3 AU due to the resolving power of imaging programmes. If works with samples with separation under 3 AU are included the total binary fractions for VLM stars and brown dwarfs (BDs) could range between 2-50% (Bardalez Gagliuffi et al. 2014). These differences can be due either to a continuous formation mass-dependent trend or to differences in the formation mechanism of the VLM objects.

Wide (> 100 AU) binary companions are relatively common for high-mass stars. Raghavan et al. (2010) found that $\sim 25\%$ of solar-type stars have a companion with separations wider than 100 AU and $\sim 11\%$ wider than 1000 AU. Tokovinin & Lépine (2012) estimates that at least 4.4% of the solar-type stars have a companion at more than 2000 AU. Nevertheless, different projects dedicated to find wide VLM binaries concluded that they are rare. Allen (2007), via statistical investigation utilizing a Bayesian algorithm, found that only 2.3% of VLM objects have a companion in the 40-1000 AU range. Burgasser et al. (2009) estimated a fraction of VLM wide multiples in the field of no more than 1%-2%. For a recent review on stellar multiplicity, see Duchêne & Kraus (2013).

Searches for VLM companions to M dwarfs at large separations (> 100 AU) remain incomplete. The discovery of VLM binaries with separations of thousands AU (e.g., Artigau et al. 2007, Caballero 2007a,b, Radigan et al. 2009) point to the existence of a population of such ultra-wide systems. Dhital et al. (2010), presented the Sloan Low-mass Wide Pairs of Kinematically Equivalent Stars (SLoWPoKES) catalogue with 1342 very-wide (projected separation over 500 AU) low-mass (at least one mid-K to mid-M dwarf component) common proper motion pairs identified from astrometry, photometry, and proper motions in the Sloan Digital Sky Survey (SDSS). They found that the wide binary frequency was at least of 1.1% in the spectral types of the catalogue with many pairs so weakly bound ($\approx 10^{33}$ J for the weakest) that overcome the limits of previous empirical limits (Close et al. 2003; Burgasser et al. 2007). The catalogue also presents a bimodality in binary separation (as marked by previous works, e.g. Kouwenhoven et al. 2010), suggesting the presence of two populations, one "old" and tightly bound, with binding energies of formation to survive the age of the Galaxy and other "young" weakly bound systems, recently formed and that will not survive more than 1-2 Gyr. Janson et al. (2012) presented the results of an

extensive high-resolution imaging survey of M-dwarf multiplicity, where they found a multiplicity fraction of $27 \pm 3\%$ for M-dwarfs within the AstraLux detection range of $0.08''$ – $6''$, semimajor axes in 3-227 AU range at a median distance of 30 pc. They concluded that their results indicate a common formation mechanism between stars and BDs. Also, Baron et al. (2015) reported the discovery of 14 VLM binary systems formed by mid-M to mid-L dwarf companions with separations of 250-7500 AU.

Despite the relevant contribution of the mentioned works in the field of VLM wide binaries, the number of known pairs formed by mid to late M (or cooler) dwarfs is still small.

A compilation from the articles previously reported gives ~ 100 wide systems formed by M or later components and ~ 40 with components with M5 or later spectral types. During the writing of this paper, Dhital et al. (2015) present the second part of SLoWPoKES, that contains a significant number of binaries at the late-M spectral types. They identified 944 sdM + sdM binary candidates and 141 in which both components are VLMs, although spectroscopic data are needed to confirm them.

Recently also higher order multiplicity has also been explored as key to constrain the star formation processes. Faherty et al. (2010) found that the frequency of tight resolved binaries in wide systems (> 100 AU) that contains an UCD ($> M6$) is at least twice (50%) the frequency for wide isolated field UCDs (10-20%). They obtained values of 3:5 and 1:4 ratios of triples and quadruples to binaries respectively, in comparison with 1:4 and 1:26 ratios from Reid & Hawley (2005) M dwarfs sample. Law et al. (2010) studying a sample of 36 extremely wide (600–6500 AU) M1-M5 dwarf binaries obtained a bias-corrected, high-order-multiple fraction of 45%, with a quadruple incidence inferior to 5%. The authors reported an increase in the high-order multiple fraction for the widest targets, reaching 21% for systems with separations up to 2000 AU and 77% for systems with separations over 4000 AU. Also, Allen et al. (2012) estimated a wide tertiary fraction of 19.5% from a multi-epoch search for wide (> 200 AU) low-mass tertiary companions of a volume-limited sample of 118 known spectroscopic binaries within 30 pc of the Sun.

These wide binaries, with large separations and low binding energies, have a strong impact on the proposed formation theories. In particular, it challenges the ejection model (Reipurth & Clarke 2001; Bate & Bonnell 2005) since such fragile systems are not expected to survive the ejection process from their birth environments. They also raise some concerns on the disc fragmentation scenario (Padoan & Nordlund 2002) as such wide systems would require the existence of discs of unreasonable mass and size. The photoevaporation mechanism (Whitworth & Zinnecker 2004), on the other hand, demands the presence of nearby massive young stars, and therefore cannot be a universal mechanism for VLM multiple formation (Burgasser et al. 2007). Also the massive stars would probably disrupt the wide VLM multiple system.

Kouwenhoven et al. (2010) and (2011) remarked that wide binary systems, with separations larger than 1000 AU, could not have been formed as primordial binaries in star clusters since their orbital separation would be comparable to the size of a typical embedded cluster. They proposed,

based on N-body simulations, that these binary systems were formed during the star cluster dissolution process, since escaping stars would have very similar velocities, easing the formation of wide systems. Based on the relatively high percentage of binaries found (up to 30 %) they also predicted a high frequency of triple and quadruple systems.

The discovery of wide binaries in large regions of the sky typically requires managing huge volumes of data coming from different astronomical archives and services which, once discovered and gathered, need to be cross-matched and filtered following a number of photometric and kinematic criteria. The drawbacks associated with this type of analysis can be overcome if the work is done in the framework of the Virtual Observatory (VO¹), an international initiative whose main goal is to guarantee an easy access and analysis to the astronomical data distributed worldwide.

Making use of VO tools, we searched for wide binaries exploring the limits in distance and binding energy. We have discovered new 36 low-mass and VLM multiple systems, with averaged projected separation between ~ 200 and ~ 92000 AU, using the Two Micron All Sky Survey (2MASS) Point Source Catalogue (PSC; Skrutskie et al. 2006), the Sloan Digital Sky Survey (SDSS) Data Release 9 (DR9) Photoprimary Catalogue (Adelman-McCarthy et al. 2009), the Large Area Survey of the United Kingdom Infrared Telescope Infrared Deep Sky Survey Data Release 10 (UKIDSS LAS DR10; Lawrence et al. 2007), the Wide-field Infrared Survey Explorer (*WISE*; Wright et al. 2010), and The Galactic Legacy Infrared Mid-Plane Survey Extraordinaire (GLIMPSE²) data bases. Also, we have found 50 low-mass objects with $\sim L0$ - $T2$ photometric spectral types. Only one of these objects presents a common proper motion high-mass companion, inside our research limits. The methodology is outlined in Section 2, while Section 3 describes the proper motions. Sections 4 and 5 present the analysis of general properties of the new systems and of the L dwarfs respectively. Section 6 presents the search of high-mass companions. Section 7 presents the discussion of results and the summary and conclusions are given in Section 8.

2 SEARCH METHODOLOGY

We searched for common proper motion objects with colours consistent with spectral types later than M0, using STILTS³ to build a workflow consisting of the following steps:

- **Cross-matching:** We performed a cross-match between the 2MASS and the SDSS DR9 Catalogues in the whole area of the sky covered by SDSS (≈ 14555 squares degrees). We used the command *tskymatch2* with the option *best*. This makes a crossmatch of two tables based on the proximity of sky positions. The best pairs were selected in a way which treats the two tables symmetrically. Any input row which appears in one result pair was disqualified from appearing in any other result pair, so each row from both input tables appears in at most one row in the result. We used a matching radius of $10''$ to ensure that objects with high proper motion

are not left out and, at the same time, keep the management of false alarms tractable. Considering the maximum possible time difference between 2MASS and SDSS observations (12 years, 1997-2009), a separation of $10''$ implies that we are able to find all objects with proper motions less than $0.8''/\text{yr}$. Faherty et al. (2009), in their kinematic study of late-type dwarfs, concluded that only $\approx 10\%$ of M dwarf have proper motions higher than $0.8''/\text{yr}$, which confirms the high level of completeness of our criterion. Only the pair 2MASS-SDSS with the minimum separation was considered. We also checked that this pair coincides with the closest SDSS-2MASS pair. Finally, given the poorer 2MASS spatial resolution compared to SDSS, we required that each 2MASS source matched a unique SDSS source within $6''$.

Using similar criteria, we also required the presence of a UKIDSS LAS (DR10) counterpart at less than $20''$ from the 2MASS source fulfilling a *ppErrbit* quality flag smaller than 256 and class star parameter *mergedClass*=-2, -1. In those sky regions not covered by UKIDSS, AllWISE⁴ was used instead. To ensure a real displacement of the source between the 2MASS and UKIDSS (*WISE*) images we required a separation 2MASS-UKIDSS (2MASS-*WISE*) larger than $0.7''$ (the 90 percentile in separation using all objects in the image is typically $\approx 0.6''$).

- **Filtering:** The sources obtained from the cross-match were filtered using the following criteria:

- $X\text{flg}=0, A\text{flg}=0$, to avoid sources flagged in 2MASS as minor planets or contaminated from nearby extended sources.

- $J \leq 17$, to get rid of too faint objects which typically have associated large photometric uncertainties.

- $Q\text{flg}(J) \neq "U"$, to discard sources with upper limits in the *J* band.

- **Photometric cuts:** we kept objects fulfilling the following colour criteria:

- Objects with M spectral type (West et al. 2011):
 $(0.48 \leq (r - i) \leq 2.90) \wedge ((0.27 \leq (i - z) \leq 1.89)$
 $\& r < 22.2 \& i < 21.3 \& z < 20.5$

- Objects with L-T spectral types (Schmidt et al. 2010):

- $(z - J) \geq 2.0 \& z < 20.5 \& ((i - z) \geq 1.7 \parallel i > 21.3) \&$
 $((i - J) \geq 3.1 \parallel i > 21.3)$

- **Proper motion cuts:** we required that the sign of the proper motion calculated using 2MASS-UKIDSS (2MASS-*WISE* in those regions not covered by UKIDSS) both in RA and DEC was the same of the proper motion derived using 2MASS-SDSS. This check in the two components allowed us to discard a significant number of false companions having a proper motion with a similar modulus but moving in different direction in the space.

We selected objects fulfilling the above criteria and differing $< 30\%$ in each component of the proper motion ($\mu_\alpha * \cos\delta, \mu_\delta$) (see Sect. 3) and $< 20\%$ in distance (see Sect. 4). Although the common proper motion criterion may look rather conservative compared to other criteria found in the literature (typically $\Delta\mu/\mu < \sim 0.2$: see, for instance, Dupuy

¹ <http://www.ivoa.net>

² <http://www.astro.wisc.edu/glimpse>

³ <http://www.star.bris.ac.uk/~mbt/stilts/>

⁴ <http://cdsarc.u-strasbg.fr/viz-bin/Cat?II/328>

& Liu 2012), we note that the great majority of the common proper motion pairs given in Tables 1 and 2 fulfill this relation and even $\sim 40\%$ have $\Delta\mu/\mu < 0.1$. We also imposed a condition on separations, rejecting system with angular separation smaller than $1''$ and larger than 100,000 AU. Finally, the remaining candidates were visually inspected to eliminate artifacts and spurious matches. The search of companions was performed in steps, where the sky was divided first in one square degree fields in which all the criteria were applied and with the final output of total candidates. We therefore have not kept the intermediate numbers, objects per field, although it will give a rough estimation that the search was performed around $\sim 100,000$ objects in all sky covered by SDSS.

This way we ended up with 39 candidate pairs and three objects candidates to form a triple system (Table 1) in the area common between 2MASS (PSC), SDSS (DR9) and UKIDSS LAS (DR10). The 40 systems are form by components with $\sim M0-L0$ photometric spectral types. Six of these candidates were previously identified in the Washington Double Star Catalog (WDS; Manson et al. 2001) and one in the recently released SLoWPoKES-II. All of them were removed from our list. In those regions not covered by UKIDSS we identified six candidates to binary/multiple systems in the area in common between the 2MASS, SDSS, and *WISE*. One remaining candidate was found as byproduct using 2MASS, *WISE* and GLIMPSE positions. These seven systems have components with $\sim M0.5-L0$ photometric spectral types. One of them is candidate to a triple system (Table 2). From this list, four objects previously identified in the WDS catalogue were also removed. No candidate to binary/multiple system were found with spectral types later than L0. As part of our analysis we also identified 50 new L-T candidates according to our photometric cuts, with no low-mass proper motion companion inside the settled constraints (Table A1).

Finally, we ended up with 36 pair/multiple identified as potential common proper motion objects. Additional eleven pairs were previously reported in SLoWPoKES II (1) and in the WDS catalogue (10). We kept them in our list to improve their physical parameters. In particular, spectral types were calculated for seven of them for the first time. None of our 36 systems were found in Slowpokes I, Faherty et al. (2009; 2010), Caballero (2009), Radigan et al. (2009), Zhao et al. (2011), Luhman et al. (2012), Mužić et al. (2012), Deacon et al. (2014) or Baron et al. (2015).

Figure 1 displays the spatial distribution of our candidate list compared to SLoWPoKES.

3 COMMON PAIRS

3.1 Proper motions

Proper motions were calculated from the differences in position between the 2MASS, SDSS and UKIDSS epochs for a list of targets that we call group A and between the 2MASS, SDSS and *WISE* for a list that we call group B. Whenever possible, other catalogues (the first and the second Palomar Observatory Sky Survey (POSS-I and POSS-II), GLIMPSE, etc) were used to add new epochs and improve the calculated values. The proper motion of each component was calcu-

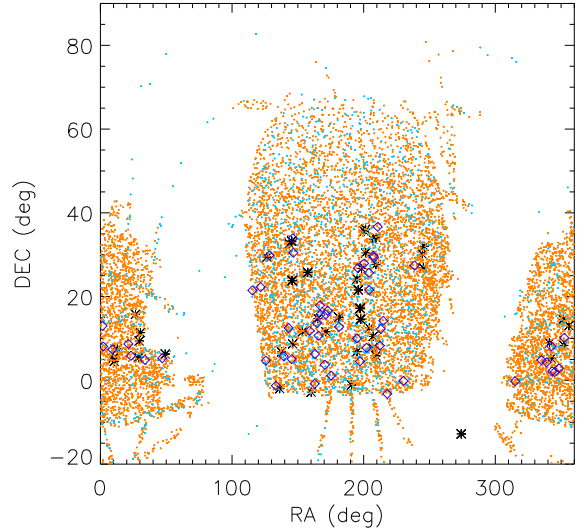


Figure 1. Spatial distribution of the binary (black asterisks) and L dwarf (dark blue diamonds) candidates compared to that of SLoWPoKES binaries (orange small crosses) and SLoWPoKES VLM binaries (light blue small crosses).

lated in the standard way by single least squares fit to all the available positions.

The positions for each system component in 2MASS, SDSS and UKIDSS/*WISE* catalogues are given in Tables 1 and 2. Final proper motions are given in last two columns of the Tables, in $[\mu_\alpha * \cos\delta, \mu_\delta]$ format for proper motion components in column 8 and total proper motion in column 9 with the error from the fit rounded to the nearest whole number in parenthesis, both in mas yr^{-1} . Figure 2 shows a comparison between our determination of proper motion and that of some literature sources. We see how good agreement is reached in all cases with 2MASS and UKIDSS measurements although some dispersion is found with the SuperCosmos Sky Survey (Hambly et al. 2001a, 2001b, 2001c) and Position and Proper Motion Extended-L catalogue (PPMXL; Roeser et al. 2010) measurements. The values we obtained for the SLoWPoKES II and WDS objects are in agreement with the correspondent catalogue results, except for 2MASS J13104398+1434338 / 2MASS J13104431+1434326 pair for which no proper motion is given in the WDS catalogue. The highest proper motions found in our list of objects is $\approx 0.4''/\text{yr}$.

As our nearest pair is at ~ 26 pc (Table 4), we assume that the error produced by parallax in the proper motion measurements is negligible.

3.2 Astrometric confirmation

To further assess the reliability of the proper motions of the binary systems, we measured the variation of the angular separation, ρ , and orientation or parallactic angle, θ , defined as $\theta = \text{atan}(\delta(RA)/\delta(DEC))$, between the components of each pair. Five epochs (POSS-I, POSS-II, 2MASS, SDSS, UKIDSS) or a span of ~ 50 years were available for 31 pairs, four epochs (POSS-II, 2MASS, SDSS, UKIDSS) or about 20 years of time base-line for 6 pairs and three epochs (2MASS,

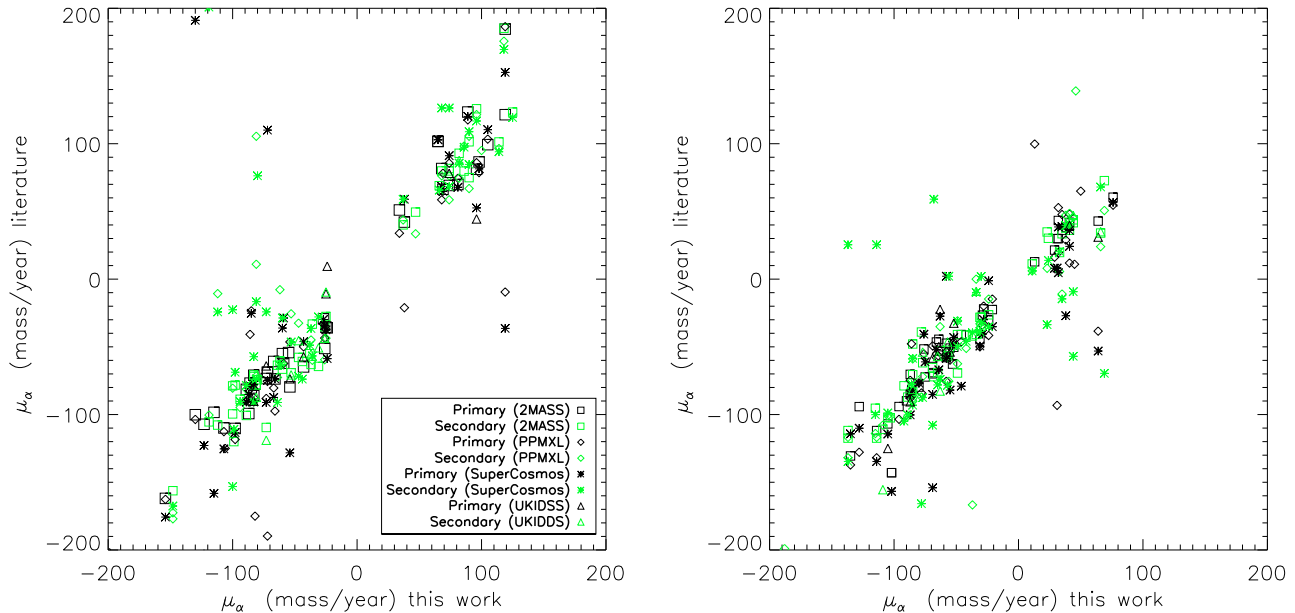


Figure 2. Comparison of proper motion measurements with literature sources. Primaries and secondaries are in black and green character, respectively.

SDSS, UKIDSS) or a coverage of ~ 10 years for 3 pairs. Note that the 36 systems are formed by 34 binaries and 2 triples, what gives a total of 40 pairs considering the components of the two triples in pairs. If the pairs are real common proper motion objects, ρ and θ should remain constant within the errors. To check this, we compared the mean value of ρ and θ with the values that these parameters should have if the second component of the system was a fixed, background star. We assumed common proper motion provided that the difference in ρ and θ is higher than 3σ for time baselines of 50 years, 2σ for epochs separated 20 years and 1σ for baselines of 10 years. All systems fulfilled these criteria.

3.3 Chance alignments

The probability of random alignment is the probability that, for chance, in a search like ours, we find physically unrelated stars having the same proper motion and distance within our uncertainties. The probability is calculated by multiplying the probability of finding two stars with the same proper motion by the probability of finding two stars at the same distance.

We looked for PPMXL sources with the same proper motion within the assumed uncertainties (difference of less than 30% in both components) in a cone of $10'$ radius (slightly larger than the largest separation between components) centred in every candidate system. We found that the probability of a single star having a common proper motion occurring by chance is $\sim 0.15\%$.

In a second step, we used the space density of M dwarfs ($\approx 5.4 \times 10^{-2} \text{ pc}^{-3}$, from Caballero et al. 2008 and reference therein), to estimate the likelihood of a close proximity in space by chance. Taking into account the distances and the separations of our system, we calculated a volume for each target. The probability of sharing by chance the same vol-

ume of space, calculated as $\text{density} \times \text{volume}$ or, equivalently, assuming Poisson statistics ($P = 1 - e^{-\rho * V}$; e.g. McElwain & Burgasser 2006), ranges from 10^{-1} to 10^{-6} .

The combination of these two factors indicates that the probability of a single star having a chance alignment in space and motion at the level of our uncertainties ranges from 10^{-3} to 10^{-9} . To get the chance alignment probability for the sample we need to sum the individual probabilities (1.2×10^{-3}), and then multiply by the number of objects searched for companions (100,000 approx.) divided by the number of objects found (96). We obtain that there might be between 1 and 2 chance alignment in our sample of 47 systems. This indicates that the majority of our candidates form physical pairs. However, we note that the wider the binary, more likely to be chance alignments because the probability of chance alignment goes up with separation.

4 PROPERTIES OF THE NEW SYSTEMS

4.1 Kinematics

True space velocities are better indicators of an object's kinematics than apparent angular motions. But we only have measurements of radial velocity for two candidates, 2MASS J13570535+3403459 and 2MASS J09332493+3232033, with values of 64.2 and -12.9 km^{-1} respectively (errors between $5\text{--}10 \text{ km}^{-1}$) from West et al. (2008). They calculated the Galactic space-velocity components (U, V, W) using photometric distance values of 179 and 180 pc (quite similar to the ones obtained here), obtaining $(-32.5, -5.0, 54.0)$ and $(8.4, 1.9, -5.4)$. The (U, V, W) coordinates of 2MASS J13570535+3403459 lay in the region of young disc population defined by Eggen (1984a,b, 1989), in the Ursa Major group area (500 Myr; King et al. 2003). For 2MASS

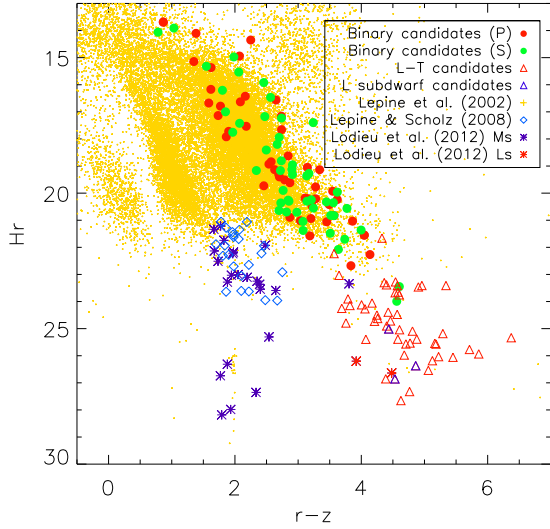


Figure 3. Reduced proper motion diagram. Small orange crosses represent all sources in Lépine et al. (2002) with counterpart in the SDSS DR7 data base (99% complete for stars with proper motions $0.5''\text{yr}^{-1} < \mu < 2.0''\text{yr}^{-1}$ down to $R=19$), blue open diamonds are known late M subdwarfs from Lépine & Scholz (2008), purple and red asterisks are M and L subdwarfs from Lodieu et al. (2012) respectively. Filled dots are our candidates to binary/multiple systems, red for primaries and green for secondaries, red triangles are the L-T candidates and blue triangles represent three L subdwarfs candidates.

J09332493+3232033, (U, V) coordinates lay also in the young disc area, but W component is situated in the field. The W component is always affected by larger dispersion, so the target may still belong to the young disc area. West et al. (2008) calculated vertical distance from the Galactic plane of 146.2 and 188.0 pc that correspond to the thin disc (e.g. Pauli et al. 2006).

For the rest of the candidates, we just made the kinematic study using reduced proper motions. Since subdwarfs are old and tend to exhibit halo or thick disc kinematics (Gizis 1997), the reduced proper motion diagram represents a useful tool to separate dwarfs from subdwarfs and white dwarfs objects (Jones 1972, Evans 1992, Salim & Gould 2002, Lépine & Shara 2005; Burgasser et al. 2007, Lodieu et al. 2012). We have used the diagram of reduced proper motion in r magnitude versus $(r - z)$ SDSS colour as in Lodieu et al. (2012). From this diagram, Figure 3, we can confirm that individual components of the systems are consistent with solar-type dwarfs of the disc population.

4.2 Properties from photometry

4.2.1 Distances

Photometric distances were calculated using the colour-absolute magnitude relations given in Bochanski et al. (2010; Table 4) for M0-M9 dwarfs. We used the $M_r - (r - z)$ relationship whenever possible and $M_r - (r - i)$ or $M_r - (i - z)$ otherwise. The associated uncertainties are $\sigma_M = 0.394$ mag, 0.403 and 0.481 mag (Bochanski et al. 2010; Table 4) which translate into errors of $\sim 20\%$ in distances. Since the pair

2MASS J18163409-1246310 and 2MASS J18163485-1246421 do not have an SDSS counterpart, we used the M_J -spectral type relation in Hawley et al. (2002) to estimate their distances. The error in distance associated with this calibration is not larger than 25%. The calculated values are given in column 7 of Tables 3 and 4.

4.2.2 Establishing these objects are dwarfs

We used Lépine & Gaidos (2011) photometric criterion to separate M dwarfs from giants and verify the dwarf nature obtained from kinematics:

$$M_V > 2.2(V - J) - 2.0 \quad (1)$$

where V magnitude was calculated for our objects using the following transformation between the SDSS and Johnson photometric systems⁵.

$$V = g - 0.5784(g - r) - 0.0038 \quad (2)$$

All our M spectral type candidates fulfilled the dwarf condition. Since 2MASS J18163409-1246310 and 2MASS J18163485-1246421 do not have SDSS colours, we used the equations (9)-(13) of Lépine & Gaidos (2011) instead to confirm their dwarf nature.

4.2.3 Effective temperatures, surface gravities and masses.

Effective temperatures and surface gravities were computed using VOSA⁶ (Bayo et al. 2008), assuming solar metallicity (as expected from dwarfs in the thin disc). VOSA is a VO tool designed to determine physical parameters from comparison of observed photometry gathering from different services (2MASS, SDSS, UKIDSS, *WISE*,...) with different collections of theoretical models. In particular, we used the BT-Settl models (Allard, Homeier & Freytag 2011, 2012) and the two methods of comparison with models that VOSA offers, namely, a χ^2 minimization, that returns the overall best-fitting model and a Bayes analysis giving information on the marginalized probability distribution of the individual parameters in the fit. In all cases, the T_{eff} obtained with the best χ^2 fit has a normalized probability larger than 0.8. This was the condition we imposed to consider the derived effective temperature reliable.

We limited the range of $\log g$ in the VOSA fitting to $\log g = 4.5-6.5$, to include the typical values for M dwarfs with ages of 0.1-10 Gyr (Jones et al. 1996) plus 0.5 dex of error. VOSA also provides mass estimations, using BT-Settl models (Allard et al. 2011, 2012). An average uncertainty of $\approx 0.015 M_\odot$ was assumed.

We also calculated masses from the M_r , M_i and M_z absolute magnitudes given in Table 5 of Kraus & Hillenbrand (2007). They adopted effective temperatures from models of Luhman (1999) for spectral types $> M0$ and then combined these T_{eff} values with the 500 Myr isochrones of Baraffe et al. (1998) to estimate stellar masses. Since 2MASS J18163409-1246310 and 2MASS J18163485-1246421 lack SDSS colours, we used the relation from J magnitude. Since theoretical

⁵ <https://www.sdss3.org/dr8/algorithms/sdssUBVRITransform.php>

⁶ <http://svo2.cab.inta-csic.es/theory/vosa/>

models can underpredict masses (e.g., Hillenbrand & White 2004; López-Morales 2007), they increased the masses of M1 stars by 5%, M2 stars by 10%, and later type stars by 20%, getting mass values more consistent with the observations. See Kraus & Hillenbrand (2007) for further details. VOSA masses are in average $0.06 M_{\odot}$ smaller than masses from Kraus & Hillenbrand (2007). In following calculations, we used the masses derived from Kraus & Hillenbrand (2007) calibration when VOSA values were not available.

The calculated T_{eff} , $\log g$ and masses are given in Tables 3 and 4. An example of VOSA fitting is plotted in Figure 4.

The masses calculated for five components in four of our systems are in the $0.06\text{--}0.07 M_{\odot}$ range, what marks the substellar limit. BDs are substellar objects, that do not have enough mass for hydrogen burning, and burn deuterium instead. With masses under $0.06\text{--}0.07 M_{\odot}$, they can not achieve the temperature needed to destroy lithium (Rebolo et al. 1996; Chabrier & Baraffe 2000; Basri et al. 2000). Lithium is so preserved independently of the objects age unlike VLM stars. But young VLM stars that still have not deleted their lithium content may be mistaken with BDs. By knowing the age of the object and if they present lithium or not, a BD can be discriminated from a young VLM object. Therefore, without age or lithium information, we have to consider that some of the five candidates may be BDs.

4.2.4 Spectral types

To infer the spectral types, we used the relation between $(r - z)$ colour index and spectral type given in Table 2 of West et al. (2011). Since 2MASS J18163409-1246310 and 2MASS J18163485-1246421 do not have SDSS colours, we used $(J - K_s)$ relation instead, and calculate the distances from the spectral type derived (see Sect 4.2.1).

Two candidates have spectral classification from literature, 2MASS J13570535+3403459 and 2MASS J09332493+3232033, both classified as M6 by West et al. (2008) using the HAMMER stellar spectral-typing facility (Covey et al. 2007) on their SDSS spectra. These values are in agreement with our photometric spectral types (M7 and M6.5, respectively).

The spectral types from SLoWPoKES for 2MASS J01463861+1545371 / 2MASS J01463893+1545360 (M4+M4) and from WDS for 2MASS J13104398+1434338 / 2MASS J13104431+1434326 (M7+M8) and 2MASS J22492429+0517137 / 2MASS J22492577+0516592 (M4+M6) are in agreement with our classification. The spectral type in WDS for 2MASS J18163409-1246310 / 2MASS J18163485-1246421 is given as +K:, while we obtained M2+M4.5.

Spectral types are given in column 2 of Tables 3 and 4. They were used to identify the primary components of the systems, defined as those with the earliest spectral type.

4.3 Properties from spectroscopy

To complement the photometric analysis of our candidates we got spectra for some candidates and searched for available spectroscopic information in public archives.

4.3.1 Observations

For the pair 2MASS J18163409-1246310 and 2MASS J18163485-1246421, we got in service mode a LIRIS (Long-slit Intermediate Resolution Infrared Spectrograph; Manchado et al. 1998) J band spectra, at the 4.2 m William Herschel Telescope (WHT), in La Palma Observatory. The spectra were obtained on July 11th 2011 with a clear sky and a seeing of $1.5''$, and were reduced in the standard way (sky subtraction, flat-field division, extraction of the spectra and wavelength calibration) with IRAF⁷. The spectra have a wavelength coverage of $1.17\text{--}1.30 \mu\text{m}$ with a resolving power $\lambda/(\Delta\lambda) \approx 2000$. The signal to noise is ~ 70 and ~ 40 for each component at $1.2 \mu\text{m}$. We could not make a flux calibration of the data. The spectra, normalized to unity, are displayed on left side of Figure 5.

We also obtained optical spectra for both components with the TWIN spectrograph mounted on the Calar Alto 3.5 m telescope on 26 August 2012 in service mode. Weather conditions were photometric and transparency was excellent with a seeing of 1 arcsec. The TWIN spectrograph is equipped with a 2048×800 pixel CCD detector. We used the T11 low-resolution grating with a slit of 1 arcsec in the red arm, covering the $5500\text{--}11000 \text{ \AA}$ wavelength range with a resolution of 1000 \AA . We installed the T13 grating in the blue arm to cover the $3500\text{--}5500 \text{ \AA}$ range although it offers limited use for this particular study. We took one exposure of 600 sec. Both components were placed on the slit. We reduced these optical spectra in a standard manner, using IRAF. We subtracted the bias and divided by the normalized internal flat taken just after sunset. Then, we extracted optimally the one-dimensional spectrum of each component in both systems. We calibrated our spectra in wavelength with the Helium-Argon lamps taken before sunset to an accuracy better than 0.1 \AA . Finally, we calibrated the extracted spectrum of each component with a spectrophotometric standard (HZ44; Oke 1990) observed for this programme. The flux calibration is only valid up to $\sim 9000 \text{ \AA}$, where flux is well characterized. The spectra, normalized at 7500 \AA , are displayed on right side of Figure 5.

In parallel to this, we looked for additional spectroscopic information available in public archives. Only five spectra were found, all of them in the SDSS data base⁸: 2MASS J09332493+3232033, 2MASS J09425716+2351200, 2MASS J13090058+1709066, 2MASS J13092549+1714584 and 2MASS J13570535+3403459. The spectra have a wavelength coverage of $3800\text{--}9200 \text{ \AA}$ with a resolving power $\lambda/(\Delta\lambda) \approx 1800$. The spectroscopic data are automatically reduced by the SDSS pipeline software. The spectra, normalized at 7500 \AA , are displayed in Figure 6.

4.3.2 Spectral types

In the TWIN optical spectra we estimate spectral types by using the PC3 index as defined in Martín et al. (1999). We obtained spectral types M4-5/M5

⁷ IRAF is distributed by the National Optical Observatory, which is operated by the Association of Universities for Research in Astronomy, Inc., under contract with the National Science Foundation.

⁸ <http://skyserver.sdss.org/dr10/en/tools/search/SQS.aspx>

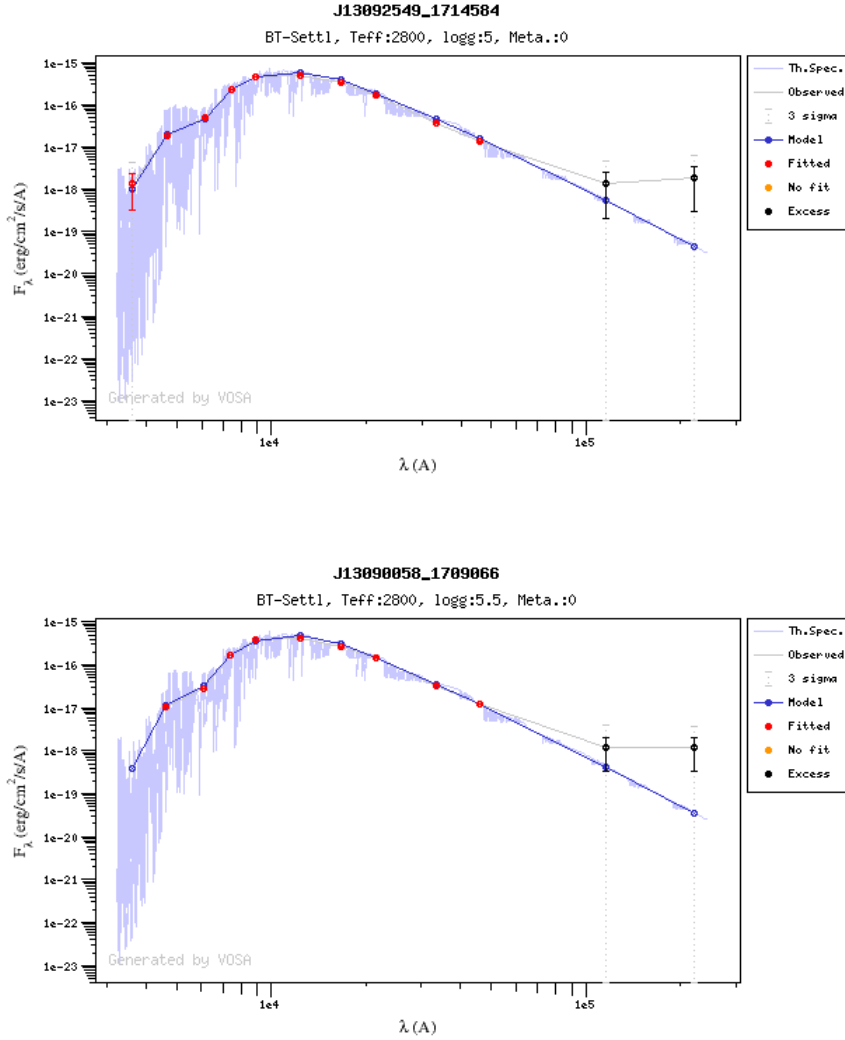


Figure 4. SED fitting plot generated by VOSA for one of the binary systems. Temperature, $\log g$ and metallicity of the best fit model are given. Blue line and dots represent theoretical spectra and photometry, respectively while red dots, joined by a grey line, represent observed photometry (SDSS, 2MASS, UKIDSS and *WISE*). Orange dots are photometric points that were not included in the fitting process. See Sect. 4.2.3 for details.

for 2MASS J18163409-1246310/2MASS J18163485-1246421. While 2MASS J18163409-1246310 shows slightly later spectral type from PC3 than from photometry, 2MASS J18163485-1246421 is in good agreement (see Table 4).

For LIRIS data, we could not make a flux calibration, therefore in order to get a spectral classification, we measured the EW of K I doublets ($1.168\mu\text{m}$, $1.177\mu\text{m}$ and $1.243\mu\text{m}$, $1254\mu\text{m}$), Na I line ($1.268\mu\text{m}$), Al I doublet ($1.311\mu\text{m}$, $1.314\mu\text{m}$) and Fe I line ($1.189\mu\text{m}$) when possible and compared them with Mclean et al. (2003, 2007) EW diagrams and tables. 2MASS J18163485-1246421 has a noisy spectrum, but we could measure some EW s. This comparison only allows us to determine that both components are earlier than M6 spectral type, which is consistent with the spectral types obtained from the TWIN spectra.

For the SDSS data, the SDSS pipeline uses HAMMER (Covey et al. 2007) to assign spectral types by measuring

a suite of spectral indices and performing a least-squares minimization of the residuals between the indices of the target and those measured from spectral type standards. The typical spectral type error is $\sim 0.5\text{--}1.0$ subtypes.

The spectroscopic spectral types are provided in Tables 3 and 4. We can see how they are compatible, within the uncertainties, with the information found by the photometric colours and the temperatures estimated by SED fitting.

4.3.3 Activity

Figure 6 presents the SDSS spectra (left) with a zoom in $H\alpha$ region (right), that can be seen clearly in emission for most of them.

We measured $EW(H\alpha)$ in the SDSS spectra, finding values of 8.2 (6.63 ± 0.049 by West et al. 2008),

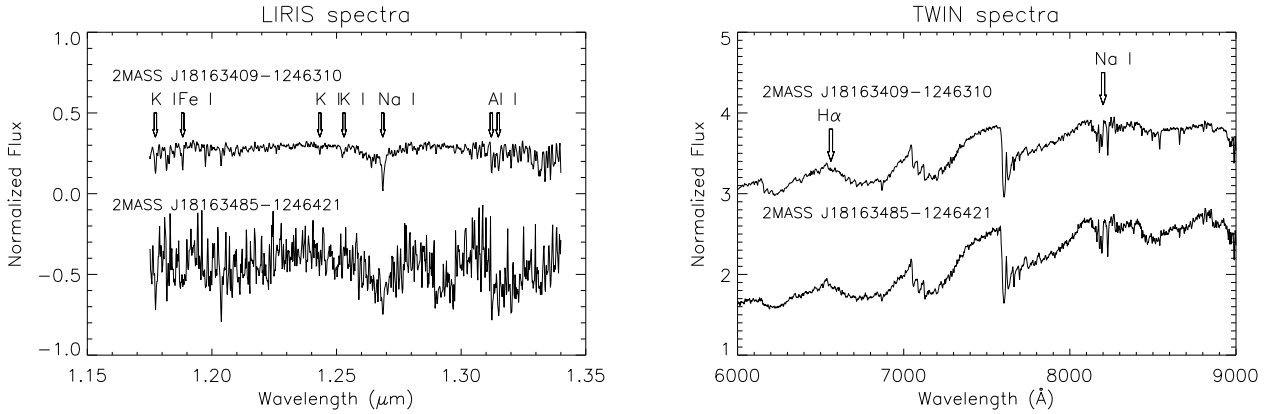


Figure 5. Observed spectra of the pair 2MASS J18163409-1246310 and 2MASS J18163485-1246421. Left: LIRIS IR spectra (normalized to unity and shifted for clarity). Right: TWIN optical spectra (normalized at 7500 Å and shifted for clarity). Some photospheric lines (see Sect. 4.3) are marked in the figure.

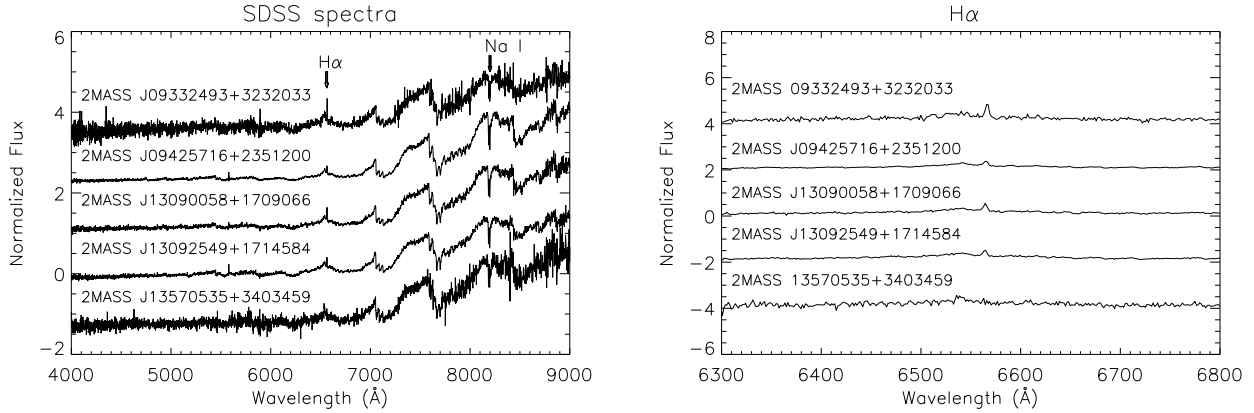


Figure 6. SDSS optical spectra (normalized at 7500 Å and shifted for clarity) of 2MASS J09332493+3232033, 2MASS J09425716+2351200, 2MASS J13090058+1709066, 2MASS J13092549+1714584 and 2MASS J13570535+3403459. Hα is seen in emission in all except for 2MASS J13570535+3403459 (zoom in the right side). Na I doublet ($\lambda\lambda$ 8183, 8199 Å) is also marked.

5.5, 4.7, 4.3 Å for 2MASS J09332493+3232033, 2MASS J09425716+2351200, 2MASS J13090058+1709066, and 2MASS J13092549+1714584 respectively, and no emission for 2MASS J13570535+3403459, although the line appears to be filled-up (West et al. 2008 give a value of $EW(H\alpha) = 0.46 \pm 0.71$). Taking into account the empirical upper limit boundary of chromospheric activity derived by Barrado y Navascués & Martín (2003), our $EW(H\alpha)$ measurements are under the dividing line between chromospheric activity and disc accretion (see e.g. Valdiolisi et al. 2009; Aberasturi et al. 2014).

Since TWIN spectra have low resolution, we could not measure $EW(H\alpha)$ for 2MASS J18163409-1246310 and 2MASS J18163485-1246421.

4.3.4 Ages

Following Table 2 in West et al. (2008), M5-M7 spectral type objects present activity lifetimes of about 7-8 Gyr. Since that is an ample range, to further constrain ages of the objects where we could measure a value of $EW(H\alpha)$ (2MASS J09332493+3232033, 2MASS J09425716+2351200, 2MASS

J13090058+1709066, and 2MASS J13092549+1714584), we compare these values and the respective spectral types with the samples in Shkolnik et al. (2009) and Gálvez-Ortiz et al. (2014). A rough estimation associates the target activity level with an age of ≈ 100 -600 Myr. In the case of 2MASS J09332493+3232033 we also have some kinematics from West et al. (2008) that may indicate an older age. The only case in which we have the spectra of both components with $EW(H\alpha)$ are for the 2MASS J13090058+1709066 / 2MASS J13092549+1714584 pair. They show similar range age, 400-600 Myr, what may confirm they formed at the same time, but 2MASS J13090058+1709066 is classified as M7.5 and therefore the activity-age relation is in the limit of applicability.

In the case of 2MASS J18163409-1246310 / 2MASS J18163485-1246421, the lack of Hα emission may indicate an old age, although Martín et al. (2010) showed that for an object with a spectral class between M6 and L4 its detection is not required to be classified as young.

We also studied the Na I doublet (λ 8183, 8195 Å) for all spectra and K I doublets (1.168μm, 1.177μm and 1.243μm, 1.254μm) for 2MASS J18163409-1246310 /

2MASS J18163485-1246421 pair. Schlieder et al. (2012) presented a study of the Na I doublet EW s in giants, old dwarfs, young dwarfs, and candidate members of the β Pic moving group using medium resolution spectra. They concluded that the Na I doublet can be used as an age indicator for objects with spectral types later than M4 and younger than 100 Myr, where metallicity has an important role. Other similar studies used the sodium diagnostic to discriminate objects up to 200 Myr (e.g Barrado y Navascués 2006, Gálvez-Ortiz et al. 2014). We measured the Na I pseudo-equivalent widths, $EW=5.6/7.0/6.8/5.8/7.2/6.2/7.2$ Å, for 2MASS J18163409-1246310, 2MASS J18163485-1246421, 2MASS J09425716+2351200, 2MASS J13092549+1714584, 2MASS J13090058+1709066, 2MASS J09332493+3232033 and 2MASS J13570535+3403459, suggesting ages older than ~ 200 Myrs (Martín et al. 2004, see Table 2 and Figure 4 therein; Schlieder et al. 2012; Gálvez-Ortiz et al. 2014, Table 10). Differences in metallicity and measurements in different resolution spectra, lack of homogeneity, etc, should be taken into account when assessing the results of these comparisons. In the 2MASS J18163409-1246310 / 2MASS J18163485-1246421 pair, the K I lines seem to be weaker than expected for an object with the spectral type estimated using photometry. This could be an indicator of low gravity (and, therefore, youngness). Nevertheless this result must be taken with caution based on the low S/N of the spectrum and the discrepancies found between the spectroscopic and photometric spectral types.

Further spectral characterization where age estimation could be derived for each system component could state if a pair has formed at the same epoch and therefore enlighten the formation processes of these wide low-mass systems.

4.4 Orbital period

Because of projection effects, the real separation between components is expected to be, on average, 1.4 times larger (Cousteau 1960). But in our case, we decided to take just the average of the measured projected separation (column 9 of Tables 3 and 4), and the masses found with VOSA (column 5 of Tables 3 and 4) to estimate an orbital period for each system. If VOSA mass was not available we used the mass derived from Kraus & Hillenbrand (2007; column 6 of Tables 3 and 4). The orbital periods range from $\sim 3 \times 10^3$ to $\sim 5 \times 10^7$ years for our candidates. Therefore, none of our candidates will have measurable orbital motions and hence will have common proper motion on the sky.

4.5 Binding Energy

Low mass and VLM wide binary systems are expected to have very low (absolute values of) gravitational potential (binding) energies, $U_g = -GM_1M_2/r$ (with M_1 and M_2 the masses of each component and r the distance between them). We have calculated the binding energies for our systems using the value of masses obtained by VOSA, and the projected physical separation (instead of the true separation) and compare them with those of other low and VLM, wide separation binaries from the literature (see the last column of Tables 3 and 4 and right-hand panel of Figure 10). We consider a physically bound system when binding energy is

over 10^{33} J (Dhital et al. 2010). Nine of the system show energies under this limit though. We discuss if these candidates are bound or not in Sect.7.

5 NEWLY IDENTIFIED L-T OBJECTS

In addition to the 47 very low-mass systems, we identified 50 isolated objects fulfilling the L-T photometric cuts described in Sect. 2 and not previously reported in the literature. We measured some characteristics of these objects and included them here for future studies.

Proper motions of these targets were measured in a similar way to that described in Sect. 3. but this time using only 2MASS and SDSS epochs (Table A1, columns 7, 8). We used the position of the candidates in other catalogues (UKIDSS, *WISE*) to confirm the modulus and sign of each component of the proper motion to keep them as candidates.

Spectral types and distances were determined using the $(i-z)$ and $(i-J)$ relations with spectral type and absolute magnitude given in Schmidt et al. (2010, Table 3 and eq. 1, 2). Averaged values of spectral types and distances obtained with each colour are given in columns 8 and 11 of Table A1.

Effective temperatures and surface gravities were computed using VOSA in the same way as we did for M dwarfs (Sect. 4.2.3).

Three of the targets, 2MASS J105804+133947, 2MASS J113052+163801 and 2MASS 13084263+0432441 may correspond to low metallicity Ls, or L subdwarfs. L subdwarfs are fully convective objects representing the low mass end of the Population II objects. They retain the original chemistry of the early Galaxy and, therefore, are good tracers of the Galactic halo formation and evolution. We have marked the three targets in Table A1 with proper motion over than 150 mas yr^{-1} whose $(J-K)$ and $(z-J)$ colours follow the criteria of Lodieu et al. (2010) for the selection of this type of objects and also lay in the appropriate area of the $(i-J)$ vs $(J-K)$ diagram of Zhang et al. (2017). Moreover, although the reduced proper motion diagram (Figure 3) seems to not discriminate between dwarfs and subdwarfs in the L spectral type region, the three targets lay close to other L subdwarfs identified in the literature.

We observed two of these L subdwarf candidates (2MASS J105804+133947 and 2MASS J113052+163801) with the Optical System for Imaging and low Resolution Integrated Spectroscopy (OSIRIS; Cepa et al. 2000) instrument on the 10.4 m Gran Telescopio de Canarias (GTC) on 10 June 2015 in service mode as part of a filler programme (programme number GTC38_15A; PI Lodieu). We obtained a single on-source spectrum of 1800 sec for each candidate with the grism R500R and a slit of 1 arcsec to cover the 5000–10000 Å range. Bias, flat-field, and arc lamps were observed during the afternoon preceding the observations as part of the GTC standard calibration plan. We reduced the data under the IRAF environment (Tody 1986, 1993). We removed the median-combined bias, divided by the normalized median-combined dome flat before extracting optimally the spectrum and calibrating it in wavelength with an rms better than 0.35 Å. We found that 2MASS J113052+163801 is probably a $\sim M9$ type dwarf whereas 2MASS J105804+133947 looks like an early-L dwarf with some features indicating metallicity less than

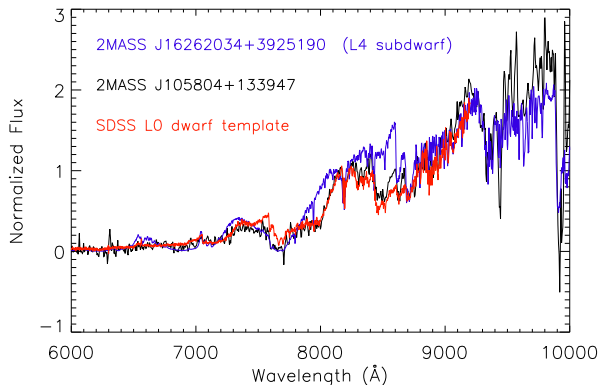


Figure 7. Comparison of 2MASS J105804+133947 spectrum with a L0 dwarf template from SDSS and a known subdwarf 2MASS J16262034+3925190 (Burgasser 2004).

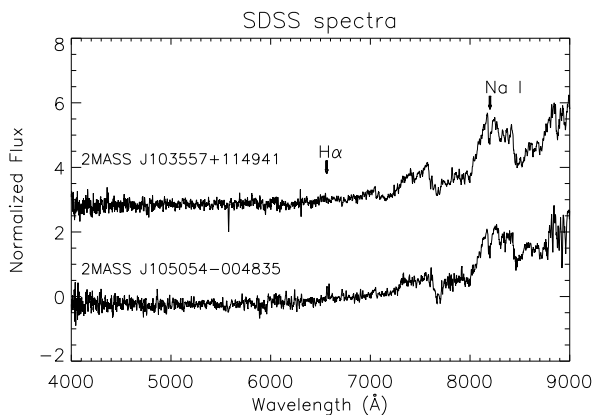


Figure 8. SDSS optical spectra, normalized at 7500 Å smoothed and shifted for clarity, of 2MASS J103557+114941 and 2MASS J105054-004835. Both are classified as L1.5. H α and Na I doublet region are also marked.

solar. Figure 7 presents a comparison of the optical spectrum of 2MASS J105804+133947 to SDSS templates of solar and low-metallicity concluding that it is most likely a dL/sdL1 \pm 1.0. Further analysis is therefore needed to confirm or not its subdwarf nature.

In the same way as for M dwarfs, we searched for available spectroscopic information in public archives. We found that two of the targets, 2MASS J10355745+1149420 and 2MASS J10505470-0048352, have a SDSS spectrum (see Figure 8). Both spectra are classified by the SDSS pipeline software as L dwarf, in agreement with our classification (see Table A1).

6 HIGHER-MASS COMPANIONS

Very low-mass objects in multiple systems with higher-mass stars are very interesting objects as their physical parameters can be accurately constrained via their primaries and, therefore, can be used for testing theoretical models of atmospheres and interiors. Also, low-mass wide binaries with

a high-mass companion will have strongest binding energy and, therefore, more probability to survive with time.

We searched for higher-mass companions to the system candidates using Tycho-2, PPMXL and UCAC4 (Fourth U.S. Naval Observatory CCD Astrograph Catalogue; Zacharias et al. 2013) catalogues. We looked for objects whose proper motions and distances differ by less than 3σ from the average values of our pairs. Separations translating into binding energies below 10^{33} J were discarded. For the search in PPMXL and UCAC4, we also add the condition $J(2MASS) < 15.5$.

With these criteria, we identified in PPMXL six objects as potential third components to five systems. Searches in Tycho-2 and UCAC4 did not return new candidates. VOSA was utilized to obtain their temperatures. We considered the masses from Gray (1992) and Kaltenegger & Traub (2009) for the spectral types in the A0V-K7V and M0-M9 ranges, respectively. We used Table 3 of Covey et al. (2007) to derive absolute J -band magnitudes and calculate distances and separations. Targets and their properties are displayed in Table 5, marked as blue dots in Figure 10 and discussed in next section.

For the other binaries, we assume that, under our search conditions, they are not members of higher multiplicity systems. Apart from the possibility of fainter or/and wider companion, it is also possible that some of our objects are unresolved binaries themselves, formed by low-mass companions of similar spectral type, and therefore with a total higher mass, making binding energies even higher than those calculated in Section 4.5.

We proceeded in a similar way and looked for possible bright companions to L-T dwarfs included in Table A1. Only one high-mass object, PPMXL 4077732287929300487, was identified as possible primary. The new system characteristics are displayed in Table 6, where we assume 0.075 M_{\odot} for the L dwarf in the binding energy calculations. The system is marked as a green dot in Figure 10 and discussed in next section.

7 DISCUSSION

The combination of the catalogues that we used in the search allows us to be 95% complete up to $r=22.2$, $i=21.3$ and $z=20.5$ (SDSS completeness) and $J=15.8$ (from 2MASS). The maximum distance at which an object will be included in the search is ~ 75 -700 pc for M dwarfs and ~ 10 -65 pc for L-T dwarfs. Given the angular separation limits of our search algorithm, we do expect to be overlooking genuine wide binaries with very large angular separations. Since we take these limits in order to keep a relative binding energy that guarantees real linkage of the components, we expect the percentage of binaries that we may miss is small. We have not attempted to account for incompleteness or bias, therefore the following discussion does not present conclusions about the population as a whole, but a comparison of our sample characteristics to the literature findings.

It is well known that the binary frequency decreases with primary mass, i.e. spectral type (see e.g. Aberasturi et al. 2014; Figure 9). Therefore the distribution of primaries (defined as the component with the earliest spectral type), should show a smooth decrement towards later spec-

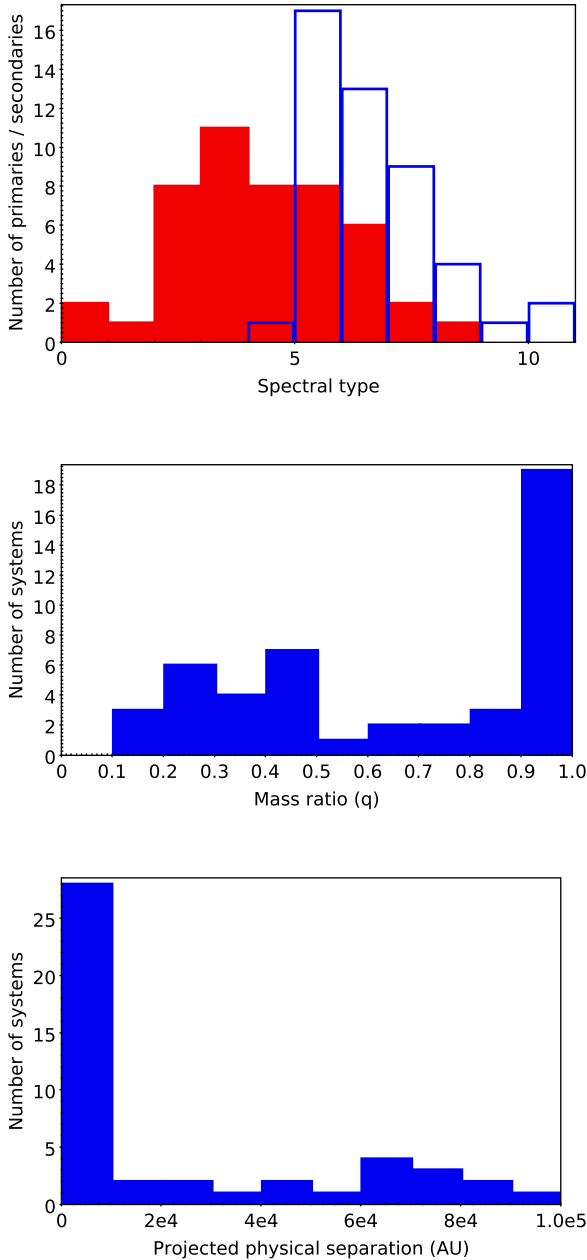


Figure 9. Top panel: spectral distribution of primaries (red) and secondaries (blue) of the objects included in Tables 1 and 2. Spectral types M0-L0 are represented by 0-10. Middle panel: mass-ratio distribution for the sample. Bottom panel: projected physical separation distribution for the sample. The sample has not been corrected for incompleteness.

tral types with a peak around M3-M4 (e.g. Farihi et al. 2005; Reid et al. 2007; Stelzer et al. 2013, and references therein). We plot in Figure 9 (top panel), the distribution of primaries (red) and secondaries (blue) for our sample. They follow the expected trend.

The mass-ratio and semimajor axis distributions for binary components provide key information about the formation mechanism of the systems. The mass ratios of binaries among Sun-like stars are distributed quite uniformly, while

for BDs a preferentially nearly equal in mass distribution is present (e.g., Burgasser et al. 2007; Raghavan et al. 2010; Bate 2012). For our small sample, we find a rather uniform distribution (Figure 9 middle panel). The peak in the 0.9-1.0 interval may reflect the presence of VLM/BD binary systems among our candidates. Also, as expected from VLM systems, the projected physical separation distribution peaks at small values ($< 10^4$ AU, Figure 9 bottom panel), with a maximum between 500-1000 AU. The shape of this histogram, showing an increasing trend after ~ 30000 AU, may indicate chance alignment contamination at larger separations. In any case the evolution of the multiplicity parameters with mass and its impact on the formation mechanisms of stars and BDs requires a statistically significant and unbiased sample and it is beyond the scope of this paper.

We plot in left-hand panel of Figure 10, a mass-separation diagram of our candidates, including previously known VLM binaries and some higher mass binaries, while in the right-hand panel, binding energy versus mass is plotted. From the 47 systems, 15 present separations in the 100-1000 AU range, 13 in 1000-10000 AU and 22 over 10000 AU. There are nine pairs with binding energies under the 10^{33} J limit.

Are these systems bound? how could they survive disruption? for how long are they going to be bound? According to Close et al. (1990) "the physical limit to the maximum separation [that] a candidate system could possibly have is the separation at which the differential Galactic force exceeds the gravitational binding force of the system". To study the systems stability, we used and compared different literature sources.

Following the Weinberg et al. (1987) work, Reid et al. (2001) and Burgasser et al. (2003) quantified different empirical relations between the maximum separation limit for VLM binaries in the field and their total mass. The lines representing these limits are plotted also in Figure 10 left-hand panel. As can be seen in the figure, Burgasser et al. (2003) is only applicable to a small number of targets in our sample (The relation is only valid for systems with $M_{tot} < 0.2 M_{\odot}$), none in the stability area, and only four are inside the stability limits marked by Reid et al. (2001). We should remark that Reid and Burgasser relations are empirical and based in samples with none or few such wide binaries, a number that increased after these works, implying maybe that they are out of date and probably too restrictive.

More recently, Dhital et al. (2010), applied Close et al. (2007) Galactic disc mass density and other updated parameters to Weinberg et al. (1987) equations. They applied the resultant equation (Dhital et al. 2010; eq.18) to describe statistically the widest binary that is surviving at a given age. In Figure 10 left panel, we overplot the lifetime "isochrones" suggested by Dhital et al. (2010) for dissipation times of 1, 2, and 10 Gyr. Twenty seven of the 51 pairs of the sample are situated over the 10 Gyr limit, eight are situated between the 2 and 10 Gyr isochrones, 12 between the 1 and 2 Gyr isochrones and four pairs are under the 1 Gyr isochrone limit.

Do these results mean that the pairs that do not accomplish the stability criteria are in the process of disruption or already separated? The answer is complicated, since for example, the age of the system would be needed. Dhital et al. (2010) find a *bimodality* in the separation of VLM bina-

ries. They argued that the finding was real and not due to any contamination or bias in the sample, and it is also predicted in recent N-body simulations (e.g. Jiang & Tremaine 2009; Kouwenhoven et al. 2010). They suggested that this bimodality reveals two distinct populations of wide binaries, possibly representing systems that form and/or dissipate through differing mechanisms (see references therein for details). Following this suggestion, we find also the possible division of our sample in two population: one tightly bound wide systems that are expected to last more than 10 Gyr, and other formed by weak bound wide systems that will dissipate within a few Gyrs.

An estimation of the system ages is, therefore, needed to finally assess if they are actually bound or already disrupted.

Other issue to discuss is the minimum binding energy that should be expected. We established a limit of 10^{33} J in our initial conditions to consider a common proper motion pair as candidate. But this restriction has been based in the typical minimum values obtained from other systems in the literature like Dhital et al. (2010). Final results give nine pairs slightly under this limit, $0.2-0.9 \times 10^{33}$ J. We decided to keep them since the error in masses could easily situate them in higher energies and take into account the existence of objects such as SE 70 + S Ori 68 pair found by Caballero et al. (2006) with 0.2×10^{33} J binding energy.

All candidate systems fulfill the same conditions of distance and proper motion (and low probability of chance alignment). Without accurate age determination, we can not state if some of them are already under disruption processes. Therefore, although contamination is expected for the widest systems in our sample, we keep them in the list of potential wide multiple systems because our main goal is to explore the most extreme regions.

Five systems may have a high-mass companion, with spectral types $\approx G7-K9$. One of these systems may be a quadruple formed by two M dwarfs and two K stars, 2MASS J09335192+3237270 (M2.0), 2MASS J09332493+3232033 (M6.5), PPMXL 4233992647964279227 (K6) and PPMXL 4234014784472339948 (TYC 2497-1059-1; K0). For 2MASS J09332493+3232033 we estimated an age of < 600 Myr, through $EW(H\alpha)$ measurement, although W component of Galactic velocity (West et al. 2008) may indicate an older age (Sect. 4.3.4). Therefore, if the objects are gravitationally linked as seems for the binding energy values, the rest of the components would have the same age. In the left-hand panel of Figure 10, the M-M system lay over the 2 Gyr isochrone while their pairing with the K components are between the 2 and 10 Gyr lifetime isochrones for dissipation times which indicates that, according to our age estimation, the system is still physically bound.

Also, in the system formed by the 2MASS J02014517+1124244 (M2.5), 2MASS J02020000+1115202 (M5.0) pair and the PPMXL 2102675187759530038 (G7), both the M-M pair and their pairing with the G object are laying on the 1 Gyr lifetime isochrone in Figure 10. Since we have no information about the age of the system, we can not confirm if their components are still bound or not.

The other pairs with tertiaries are M-M-K triples. 2MASS J11243764+1137085 / 2MASS J11242609+1139504 / PPMXL 4137926243272078734 masses and separation provide with survival times between 2 and 10 Gyrs. 2MASS J13475983+3343241 / 2MASS J13480028+3341587 lays

over the 10 Gyr isochrone while its pairing with the PPMXL 4551655942546822025 is well over the 10 Gyr limit. 2MASS J13572013+0550251 / 2MASS J13565606+0552499 lays over the 2 Gyr isochrone and its pairing with PPMXL 4398878071445995714 is situated between the 2 and 10 Gyrs. These three systems are therefore probably still bound.

We also have the case of the L2.0 dwarf 2MASS J09320299+1231027 and the F8 PPMXL 4077732287929300487 pair. With a separation of ~ 130450 AU and a binding energy of 1.2×10^{33} J, it lays over the 2 Gyr lifetime isochrone in Figure 10. We have no information about the possible age of the targets so it might already be a dissipated pair.

8 SUMMARY AND CONCLUSIONS

Taking advantage of VO tools, we could identify 36 new low and VLM systems (M0.5-L0 spectral types) with separations in the $\approx 200 - 92000$ AU range. We also provided distances and masses of eleven pairs previously marked as binaries in the literature, giving spectral classification for seven of them for the first time and improving the classification for one of them using photometry and spectroscopy.

In the mass-separation parameter space covered by our objects (separations over 200 AU and total system masses under $1 M_{\odot}$) we have increased by 34% the number of systems previously known (Tables A2 and A3). The systems recently found by Dhital et al. (2015) were not taken into account as they require further confirmation.

From the total 47 systems, we have seven pairs formed by two low-mass objects, nine pairs formed by two VLM objects, 29 pairs formed by one low-mass and one VLM object and for the two triples, one is formed by three VLM objects and the other by one low-mass and two VLM objects. Common proper motions and distances, with negligible probability of change alignment, agree with the candidates forming a bounded pair.

Spectral types of each component were calculated using several methods. They cover the M0-L0 range, with ≈ 35 of the total 95 components in M6-M8 range. This corresponds to the transition between low-mass stars and what is called ultracool dwarfs (UCDs), characterized by a dramatic change in the spectra due to the onset of dusty condensation (Jones & Tsuji 1998).

The 2MASS J13090058+1709066 / 2MASS JJ13092549+1714584 pair masses are $0.07 M_{\odot}$ for both components. The spectra analysis in Sect. 4.3.4. allowed to estimate an age in the 400-600 Myr range, what would imply a possible BD nature of both components of the system. High enough resolution spectra to determine the presence or not of lithium in their atmospheres would help to resolve the problem of its stellar or substellar nature. A confirmed binary composed by two BDs at wide separation would provide key information and serve as test-bed for their formation and evolution theories. There are three other objects with masses in the $0.06-0.07 M_{\odot}$ range for which, without age or lithium information, is not possible to conclude about their nature.

Distances were estimated by using different relations in the literature showing a good agreement between compo-

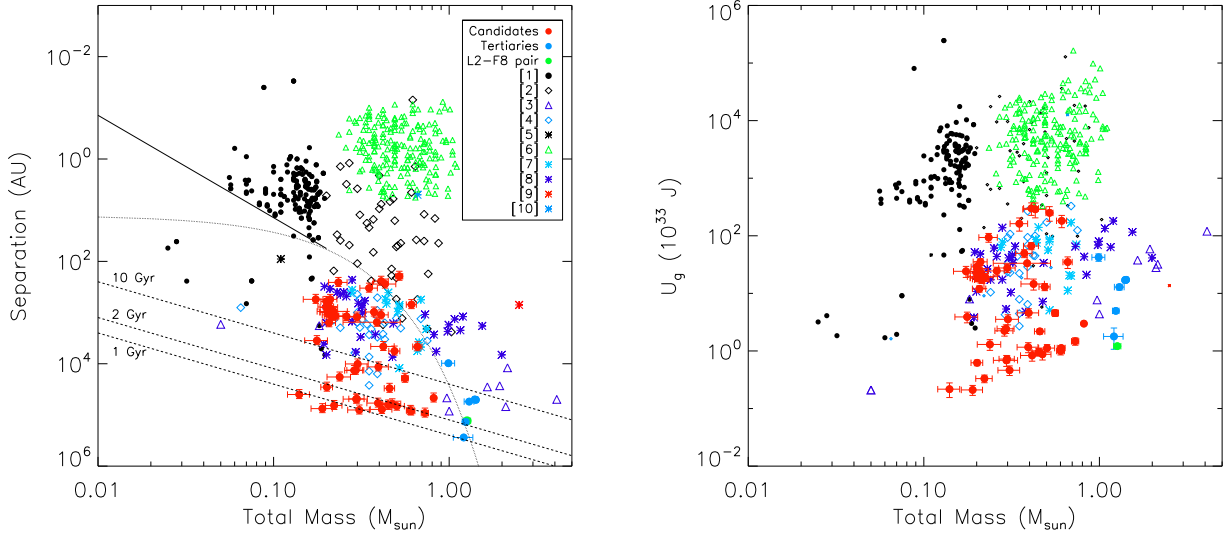


Figure 10. Separation and binding energy vs. total system mass. Known binary systems from the literature are marked with different symbols and our candidates to M-M, M-M with a higher mass companion and the only pair found for an L dwarf, are plotted with filled circles in red, blue and green respectively. In the left-hand panel we also overplot the empirical limit for stability stated by Reid et al. (2001) (dotted line) and by Burgasser et al. (2003) (solid line). We also overplot the lifetime isochrones suggested by Dhital et al. (2010) with data of Close et al. (2007) and Weinberg et al. (1987) equations for dissipation times of 1, 2, and 10 Gyr (dashed lines). Figure legend: [1]: VML archive, Burgasser et al. (2007) and Siegler et al. (2005), [2]: Fischer & Marcy (1992) and Reid & Gizis (1997), [3]: Caballero et al. (2006) & Caballero (2007, 2009), [4]: Luhman et al. (2009, 2012), Dhital et al. (2010) & Mužić et al. (2012), [5]: Burningham et al. (2010), [6]: Janson et al. (2012), [7]: Deacon et al. (2014), [8]: Faherty et al. (2010) & Baron et al. (2015), [9]: HIP 78530 AB, Lafrenière et al. (2011), [10]: Ross 458 AB, Goldman et al. (2010).

nents of each system. We calculated masses with theoretical isochrones and evolutionary models.

Although previously reported as possible binary in WDS catalogue, we could analysed in more detail the photometric properties of the 2MASS J18163409-1246310 / 2MASS J18163485-1246421 pair. Through spectroscopy we were able to obtain a reliable spectral classification for both components and measured spectral characteristics that helped to constrain the age of this pair.

We also identified 50 objects that we can photometrically classify as \approx L0-T2 spectral type and that do not present low-mass proper motion companions according to our requirements. Three of them show proper motion and photometric characteristics compatible with being low metal L subdwarfs. Two of them were spectroscopically followed-up. One was dismissed and the other one was tentatively classified as a dL/sdL11.0, with further analysis needed to confirm its subdwarf nature. This is a very interesting result given the scarce number (36) of these objects known so far.

A high-mass companion search gave us six potential companions to five of the M-M pairs and one to an L dwarf. These systems are excellent benchmarks to determine M dwarf characteristics. Many authors are actually searching for binaries consisting of an F-, G- or K-type dwarfs and an M dwarf, since high-mass companion can provide information of physical parameters (e.g. abundances) that are much more difficult and inaccurate to measure on the secondary. In future work we will follow this research line to further characterize the components of the systems with high-mass companions.

The percentage of higher-order multiple system in the

sample is rather small. We only found two multiple systems formed only by low and very low-mass components. One with components with M6.0, M7.5 and M8.5 spectral types, and other with components with spectral types M0.5, M7.0 and M8.5. With high-mass component we found five possible multiple systems, formed all of them by two Ms and a tertiary of F, K spectral types. One of them could also be a quadruple, formed by two Ms and two Ks.

Although the sample is small, we find that it follows a rather uniform distribution in mass-ratio, with an average value of 0.6 and a peak in the 0.9-1.0 interval. The semimajor axis distribution presents a peak at $> 10^4$ AU (with a maximum between 500-1000 AU).

We find that half of the sample may correspond to tightly bound wide systems that are expected to last more than 10 Gyr, and the other half to systems formed by weakly bound wide systems that will dissipate within a few Gyrs. Although we could not constrain the age of most of the candidates, probably most of them are still bound except four (2MASS J02014517+1124244 / 2MASS J02020000+1115202, 2MASS J09102559+0648533 / 2MASS J09105025+0648111, 2MASS J16183619+3005336 / 2MASS J16184068+2958293 and 2MASS J13092549+1714584 / 2MASS J13090058+1709066) formed by low-mass components whose lifetimes are ~ 1 Gyr and so maybe already under disruption processes.

The discovery of these low-mass, wide (up to 92000 AU) binary systems is a strong evidence that such systems are not as rare as was thought. The parameter space analysed here has been poorly explored before with the exception of very few papers (see references quoted throughout in this

work). Gathering an statistically significant number of wide, low and VLM systems is fundamental in order to better understand their formation and evolution processes, updating and constraining the actual theories. New, more accurate and deeper surveys are necessary to provide a realistic estimation of the population of this type of objects. Dhital et al. (2015) catalogue can provide with a good list, and soon we will have the detailed astrometrical and 3D kinematical picture of the Galaxy made by Gaia⁹, that will firmly confirm or refute the true binary nature of our candidate systems.

The VO has proved to be an excellent research methodology. In particular, it allowed an efficient management of the queries to the different catalogues and archives used in this work as well as to determine physical parameters (T_{eff} and $\log g$) through VO-tools like VOSA.

ACKNOWLEDGMENTS

M.C. Gálvez-Ortiz acknowledges the financial support of a JAE-Doc CSIC fellowship co-funded with the European Social Fund under the programme *Junta para la Ampliación de Estudios* and the support of the Spanish Ministry of Economy and Competitiveness (MINECO) through the project AYA2011-30147-C03-03 and AYA2014-54348-C3-2-R. This publication makes use of VOSA, developed under the Spanish Virtual Observatory project supported from the Spanish ministry of Education and Competitiveness (MINECO) through grant AYA2014-55216. N. L. was funded by the Ramón y Cajal fellowship number 08-303-01-02 and his research partially funded by the Spanish ministry of Education and Competitiveness (MINECO) under programmes AYA2010-19136 and AYA2015-69350-C3-2-P.

This work used observations made with LIRIS on William Herschel Telescope operated on the island of La Palma by The Isaac Newton Group of Telescopes (ING), and with OSIRIS at the Gran Telescopio Canarias (GTC) programme number GTC38_15A, both in the Spanish Observatorio del Roque de los Muchachos of the Instituto de Astrofísica de Canarias.

Also based on observations collected at the Centro Astronómico Hispano Alemán (CAHA) at Calar Alto, operated jointly by the Max-Planck Institut für Astronomie and the Instituto de Astrofísica de Andalucía (CSIC)

REFERENCES

- Aberasturi M., Caballero J.A., Montesinos B., Gálvez-Ortiz M.C., Solano E., Martín E. L., 2014, *AJ*, 148, 36
 Adelman-McCarthy J. K. et al., 2009, *Cat*, 2294, 0A
 Allard F., Homeier D., Freytag B., 2011, *ASPC*, 448, 91
 Allard F., Homeier D., Freytag B., 2012, *RSPTA*, 370, 2765
 Allen P. R., 2007, *ApJ*, 668, 492
 Allen P. R., Burgasser A. J., Faherty J. K., Kirkpatrick J. D., 2012, *AJ*, 144, 62
 Artigau E., Lafrenière D., Doyon R., Albert L., Nadeau D., Robert J., 2007, *ApJ*, 659L, 49
 Basri G., Mohanty S., Allard F., Hauschildt P. H., Delfosse X., Martín E. L., Forveille T., Goldman B., 2000, *ApJ*, 538, 363
 Baraffe I., Chabrier G., Allard F., Hauschildt P. H., 1998, *A&A*, 337, 403
 Bardalez Gagliuffi D. C. et al., 2014, *ApJ*, 794, 143
 Barrado y Navascués D., Martín E. L., 2003, *AJ*, 126, 2997
 Barrado y Navascués D., 2006, *A&A*, 459, 511
 Bate M. R., Bonnell I. A., 2005, *MNRAS*, 356, 1201
 Bate M. R., 2012, *MNRAS*, 419, 3115
 Bayo A., Rodrigo C., Barrado y Navascués D., Solano E., Gutiérrez R., Morales-Calderón M., Allard F., 2008, *A&A*, 492, 277
 Baron F. et al., 2015, *ApJ*, 802, 37
 Bochanski J. J., Hawley S. L., Covey K. R., West A. A., Reid I. N., Golimowski D. A., Ivezić Ž., 2010, *AJ*, 139, 2679
 Burgasser A. J., Kirkpatrick J. D., Reid I. N., Brown M. E., Miskey Ch. L., Gizis J. E., 2003, *ApJ*, 586, 512
 Burgasser A. J., 2004, *ApJ*, 614L, 73
 Burgasser A. J., Burrows A., Kirkpatrick J. D., 2006, *ApJ*, 639, 1095
 Burgasser A. J., Reid I. N., Siegler N., Close L., Allen P., Lowrance P., Gizis J., 2007, *prpl.conf*, 427
 Burgasser A. J., Dhital S., West A. A., 2009, *AJ*, 138, 1563
 Burningham B. et al., 2009, *MNRAS*, 395, 1237
 Burningham B. et al., 2010, *MNRAS*, 404, 1952
 Caballero J. A., Martín E. L., Dobbie P. D., Barrado y Navascués D., 2006, *A&A*, 460, 635
 Caballero J. A., 2007a, *A&A*, 462, L61
 Caballero J. A., 2007b, *ApJ*, 667, 520
 Caballero J. A., Burgasser A. J., Klement R., 2008, *A&A*, 488, 181
 Caballero J. A., 2009, *A&A*, 507, 251
 Cepa J., Aguiar M., Escalera V. G., et al. 2000, in *Society of Photo-Optical Instrumentation Engineers (SPIE) Conference Series*, Vol. 4008, *Society of Photo-Optical Instrumentation Engineers (SPIE) Conference Series*, ed. M. Iye & A. F. Moorwood, 623-631
 Chabrier G., Baraffe I., 2000, *ARA&A*, 38, 337
 Chabrier G., Johansen A., Janson M., Rafikov R., 2014, *prpl.conf*, 619
 Close L. M., Richer H. B., Crabtree D. R., 1990, *AJ*, 100, 1968
 Close L. M., Siegler N., Freed M., Biller B., 2003, *ApJ*, 587, 407
 Close L. M. et al., 2007, *ApJ*, 660, 1492
 Couteau P., 1960, *Journal des Observateurs*, 43, 41
 Covey K. R. et al., 2007, *AJ*, 134, 2398
 Deacon N.R. et al. 2014, *ApJ*, 792, 119
 Dhital S., West A. A., Stassun K. G., Bochanski J. J., 2010, *AJ*, 139, 2566
 Dhital S., West A. A., Stassun K. G., Schluns K. J., Massey A. P., 2015, *AJ*, 150, 57
 Duchêne G., Kraus A., 2013, *ARA&A*, 51, 269
 Duquennoy A., Mayor M., 1991, *A&A*, 248, 485
 Dupuy T. J., Liu M. C., 2012, *ApJS*, 201, 19
 Eggen O. J., 1984a, *AJ* 89, 1358
 Eggen O. J., 1984b, *ApJS*, 55, 597
 Eggen O. J., 1989, *PASP* 101, 366
 Evans N. W., 1992, *MNRAS*, 258, 587

⁹ http://www.esa.int/Our_Activities/Space_Science/Gaia

Table 1. Candidate position data for group A. 2MASS, SDSS and UKIDSS.

2MASS	RA_2MASS (deg)	DEC_2MASS (deg)	RA_SDSS (deg)	DEC_SDSS (deg)	RA_UKIDSS (deg)	DEC_UKIDSS (deg)	[pmRA,pmDEC] (mas yr ⁻¹)	pm (mas yr ⁻¹)
00384499+0519003	9.687477	5.316770	9.687615	5.316649	9.687654	5.316653	[81 (1), -66 (2)]	105
00391056+0525351	9.794026	5.426419	9.794192	5.426348	9.794221	5.426313	[90 (2), -49 (2)]	103
00421358+0431185	10.556616	4.521807	10.556453	4.521728	10.556358	4.521738	[-87 (23), -29 (7)]	93
00421418+0431200	10.559096	4.522232	10.558930	4.522152	10.558835	4.522159	[-89 (23), -31 (6)]	94
00513590+0735192*	12.899596	7.588668	12.899483	7.588589	12.899426	7.588535	[-43 (4), -55 (0.4)]	70
00513688+0735177	12.903701	7.588265	12.903593	7.588175	12.903535	7.588117	[-37 (5), -57 (0.1)]	68
01463861+1545371 ⁺	26.660903	15.760323	26.661022	15.760063	26.661050	15.760038	38 (1), -87 (7)]	95
01463893+1545360	26.662245	15.760003	26.662362	15.759737	26.662384	15.759711	[37 (0.3), -89 (7)]	97
01554912+0527334	28.954707	5.459282	28.954912	5.458952	28.954993	5.458881	[65 (7), -102 (13)]	121
01560037+0528494	29.001552	5.480414	29.001712	5.480140	29.001782	5.480101	[68 (8), -114 (8)]	133
01554912+0527334	28.954707	5.459282	28.954912	5.458952	28.954993	5.458881	[65 (7), -102 (13)]	121
01560053+0528562	29.002213	5.482295	29.002381	5.481999	29.002438	5.481966	[74 (2), -137 (2)]	156
01560037+0528494	29.001552	5.480414	29.001712	5.480140	29.001782	5.480101	[68 (8), -114 (8)]	133
01560053+0528562	29.002213	5.482295	29.002381	5.481999	29.002438	5.481966	[74 (2), -137 (2)]	156
01575409+0923371*	29.475390	9.393665	29.475688	9.393642	29.475735	9.393582	[89 (2), -24 (16)]	92
01575468+0923422	29.477859	9.395068	29.478163	9.395026	29.478210	9.394972	[96 (2), -30 (13)]	101
02014517+1124244	30.438228	11.406787	30.438407	11.406635	30.438435	11.406639	[74 (1), -52 (1)]	91
02020000+1115202	30.500025	11.255633	30.500192	11.255512	30.500249	11.255519	[86 (3), -42 (1)]	96
03165635+0617027*	49.234794	6.284084	49.235055	6.283981	49.235256	6.283850	[119 (2), -128 (5)]	175
03165886+0618086	49.245277	6.302416	49.245533	6.302317	49.245740	6.302179	[118 (0.3), -115 (2)]	164
08255151+2925220*	126.464651	29.422785	126.464625	29.422749	126.464542	29.422597	[-25 (1), -87 (2)]	91
08255269+2925169	126.469569	29.421366	126.469563	29.421331	126.469484	29.421178	[-25 (4), -85 (2)]	89
09045044-0158572	136.210193	-1.982583	136.210118	-1.982526	136.209978	-1.982465	[-70 (4), 76 (5)]	103
09045115-0159297	136.213158	-1.991594	136.213105	-1.991520	136.212964	-1.991452	[-73 (5), 69 (15)]	100
09102559+0648533	137.606655	6.814812	137.606631	6.814739	137.606591	6.814623	[-24 (1), -105 (7)]	107
09105025+0648111	137.709387	6.803089	137.709378	6.802990	137.709324	6.802893	[-26 (8), -109 (9)]	113
09332493+3232033	143.353891	32.534275	143.353733	32.534163	143.353651	32.534156	[-67 (5), -41 (16)]	79
09335192+3237270	143.466368	32.624184	143.466186	32.624113	143.466069	32.624054	[-83 (1), -44 (0.5)]	94
09442260+0842235	146.094169	8.706537	146.094171	8.706479	146.094379	8.706393	[119 (2), -86 (2)]	147
09442313+0842231	146.096405	8.706420	146.096413	8.706367	146.096618	8.706278	[125 (3), -85 (1)]	152
10132882+1136041	153.370110	11.601140	153.370019	11.601044	153.369914	11.600973	[-85 (3), -69 (5)]	109
10132950+1135558	153.372924	11.598843	153.372840	11.598747	153.372734	11.598678	[-81 (3), -65 (4)]	104
10402749-0248092	160.114557	-2.802568	160.114504	-2.802573	160.114337	-2.802749	[-60 (9), -56 (3)]	82
10402763-0248063	160.115158	-2.801773	160.115128	-2.801785	160.114953	-2.801964	[-59 (3), -58 (1)]	83
11002544+1445240	165.106036	14.756691	165.105892	14.756624	165.105814	14.756529	[-64 (2), -85 (5)]	105
11002578+1445299	165.107429	14.758311	165.107289	14.758234	165.107217	14.758137	[-67 (2), -76 (3)]	101
11242609+1139504	171.108715	11.664010	171.108723	11.663971	171.108969	11.663845	[82 (4), -77 (2)]	112
11243764+1137085	171.156848	11.619028	171.156953	11.618929	171.157071	11.618884	[96 (30), -63 (6)]	114
12043718+1505286	181.154927	15.091279	181.154804	15.091178	181.154646	15.091013	[-66 (4), -75 (1)]	100
12050629+1508193	181.276223	15.138718	181.276089	15.138597	181.275988	15.138506	[-94 (0.5), -86 (1)]	128
12432885-0105208	190.870227	-1.089120	190.869961	-1.089238	190.869881	-1.089241	[-99 (8), -37 (6)]	106
12433001-0105152	190.875080	-1.087576	190.874845	-1.087703	190.874763	-1.087705	[-107 (2), -31 (3)]	111

Faherty J. K., Burgasser A. J., Cruz K. L., Shara M. M.,
Walter F. M., Gelino C. R., 2009, AJ, 137, 1

Faherty J. K., Burgasser A. J., West A. A., Bochanski J.
J., Cruz K. L., Shara M. M., Walter F. M., 2010, AJ, 139,
176

Farihi J., Becklin E. E., Zuckerman B., 2005, ApJS, 161,
394

Fischer D. A., Marcy G. W., 1992, A. J., 396, 178

Gálvez-Ortiz M. C. et al., 2014, MNRAS, 439, 3890

Gizis J. E., 1997, AJ, 113, 806

Gizis J. E., Monet D. G., Reid I. N., Kirkpatrick J. D.,
Burgasser A. J., 2000, MNRAS, 311, 385

Goldman B., Marsat S., Henning T., Clemens C., J. Greiner
J., 2010, MNRAS, 405, 1140

Goodwin S. P., Whitworth A., 2007, A&A, 466, 943

Gray D. F., 1992, oasp.book.G, The observation and analy-
sis of stellar photospheres (Cambridge : Cambridge Univ.
Press), 368

Hambly N. C. et al., 2001a, MNRAS, 326, 1279

Hambly N. C., Irwin M. J., MacGillivray H. T., 2001b,

Table 1. Cont.

2MASS	RA_2MASS (deg)	DEC_2MASS (deg)	RA_SDSS (deg)	DEC_SDSS (deg)	RA_UKIDSS (deg)	DEC_UKIDSS (deg)	[pmRA, pmDEC] (mas yr ⁻¹)	pm (mas yr ⁻¹)
12593776+0651204*	194.907371	6.855669	194.907001	6.855464	194.906650	6.855262	[-372 (24), -218 (12)]	431
12593933+0651255	194.913892	6.857086	194.913513	6.856873	194.913155	6.856681	[-372 (13), -225 (9)]	434
12594856+2412318	194.952345	24.208853	194.952236	24.208815	194.952109	24.208791	[-86 (4), -28 (2)]	91
13002787+2412195	195.116132	24.205439	195.116004	24.205378	195.115911	24.205360	[-83 (1), -30 (2)]	89
13133339+2642534	198.389158	26.714849	198.389012	26.714887	198.388942	26.714966	[-72 (15), 41 (11)]	83
13133381+2642533	198.390890	26.714827	198.390766	26.714857	198.390700	26.714933	[-62 (11), 38 (9)]	72
13213074+3538472	200.378084	35.646454	200.377977	35.646372	200.377839	35.646380	[-83 (13), -24 (14)]	86
13213079+3538516	200.378323	35.647667	200.378236	35.647591	200.378078	35.647604	[-83 (13), -21 (14)]	85
13252369+3555344	201.348721	35.926247	201.348529	35.926342	201.348286	35.926386	[-119 (1), 44 (1)]	127
13253949+3604076	201.414576	36.068779	201.414368	36.068838	201.414160	36.068907	[-130 (3), 38 (0.4)]	135
13261177+3026260	201.549077	30.440556	201.548889	30.440601	201.548669	30.440698	[-123 (1), 32 (3)]	127
13261214+3026235	201.550617	30.439877	201.550429	30.439888	201.550207	30.439987	[-112 (3), 35 (5)]	117
13371237+1232212	204.301547	12.539231	204.301378	12.539181	204.301332	12.539125	[-89 (3), -46 (2)]	100
13373414+1229314	204.392287	12.492077	204.392122	12.492042	204.392081	12.491976	[-98 (4), -78 (4)]	126
13471881+0746120	206.828387	7.770011	206.828280	7.770051	206.827927	7.770095	[-154 (2), 32 (2)]	157
13471892+0746006	206.828842	7.766850	206.828751	7.766906	206.828398	7.766948	[-148 (1), 23 (4)]	149
13475983+3343241	206.999317	33.723373	206.999467	33.723156	206.999667	33.722933	[98 (3), -135 (2)]	167
13480028+3341587	207.001208	33.699646	207.001383	33.699479	207.001618	33.699302	[114 (3), -105 (2)]	155
13490345+1029167	207.264378	10.487984	207.264335	10.487902	207.264231	10.487844	[-68 (12), -71 (11)]	98
13490709+1030240	207.279556	10.506668	207.279508	10.506615	207.279419	10.506513	[-72 (2), -80 (2)]	107
13570417+2737490	209.267416	27.630281	209.267544	27.630161	209.267576	27.630020	[34 (3), -96 (1)]	102
13571335+2738194	209.305662	27.638729	209.305761	27.638622	209.305817	27.638445	[47 (13), -103 (5)]	113
13570535+3403459	209.272296	34.062771	209.272196	34.062776	209.272032	34.062807	[-82 (13), 13 (6)]	84
13570929+3403319	209.288749	34.058872	209.288578	34.058909	209.288432	34.058910	[-81 (1), 11 (5)]	82
13565606+0552499	209.233619	5.880534	209.233458	5.880416	209.233464	5.880393	[-47 (4), -63 (3)]	78
13572013+0550251	209.333897	5.840330	209.333773	5.840233	209.333700	5.840204	[-73 (2), -58 (4)]	94
16183619+3005336	244.650797	30.092670	244.650696	30.092727	244.650623	30.092792	[-27 (1), 41 (7)]	49
16184068+2958293	244.669529	29.974827	244.669449	29.974896	244.669312	29.974954	[-31 (4), 44 (3)]	54
16211986+2653207	245.332766	26.889111	245.332698	26.889148	245.332553	26.889213	[-54 (2), 64 (10)]	84
16212591+2649353	245.357968	26.826477	245.357886	26.826511	245.357677	26.826558	[-73 (10), 66 (15)]	98
16234190+3200293	245.924619	32.008152	245.924567	32.008189	245.924493	32.008230	[-27 (2), 29 (2)]	40
16241587+3155100	246.066141	31.919455	246.066076	31.919487	246.065998	31.919527	[-36 (3), 33 (2)]	49
22445443+0856474	341.226828	8.946525	341.226618	8.946404	341.226578	8.946368	[-115 (11), -53 (9)]	127
22445848+0901564	341.243695	9.032349	341.243533	9.032174	341.243495	9.032175	[-100 (9), -49 (2)]	111
22492429+0517137*	342.351209	5.287160	342.351456	5.287242	342.351458	5.287250	[105 (1), 35 (0.05)]	111
22492577+0516592	342.357384	5.283135	342.357634	5.283218	342.357639	5.283225	[90 (1), 41 (0.5)]	99
23253016+1434198	351.375679	14.572188	351.375636	14.572115	351.375524	14.571939	[-55 (2), -90 (1)]	106
23253026+1434102	351.376106	14.569505	351.376034	14.569457	351.375948	14.569287	[-38 (2), -92 (6)]	100
23280466+0821168	352.019434	8.354683	352.019330	8.354569	352.019292	8.354507	[-60 (10), -69 (6)]	92
23283688+0822011	352.153692	8.366992	352.153608	8.366903	352.153535	8.366825	[-44 (1), -69 (0.5)]	82
23433880+1304223	355.911670	13.072880	355.911867	13.072947	355.911894	13.072978	[69 (2), 31 (5)]	76
23435793+1256309	355.991385	12.941942	355.991603	12.941997	355.991618	12.942041	[66 (0.1), 24 (10)]	71

* previously found in WDS catalogue.

+ previously found in SLoWPoKES II.

MNRAS, 326, 1295
Hambly N. C., Davenhall A. C., Irwin M. J., MacGillivray
H. T., 2001c, MNRAS, 326, 1315
Hawley S. L., Gizis J. E., Reid I. N., 1996, AJ, 112, 2799
Hawley S. L. et al., 2002, AJ, 123, 3409
Hillenbrand L., White R., 2004, ApJ, 604, 741
Høg E. et al., 2000, A&A, 355, L27
Janson M., Hormuth F., Bergfors C., Brandner W., Hippler

S., Daemgen S., Kudryavtseva N., Schmalzl E., Schnupp
C., Henning T., 2012, ApJ, 754, 44
Jiang Y., Tremaine S., 2009, MNRAS, 401, 977
Jones E. M., 1972, ApJ, 177, 245
Jones H. R. A., Longmore A. J., Allard F., Hauschildt P.
H., 1996, MNRAS, 280, 77
Jones H. R. A., Tsuji K., 1998, Brown Dwarfs and Extra-
solar Planets ASP conference series, Vol 134, pg 423

Table 2. Candidate position data for group B. 2MASS, SDSS and *WISE*.

2MASS	RA_2MASS (deg)	DEC_2MASS (deg)	RA_SDSS (deg)	DEC_SDSS (deg)	RA_WISE (deg)	DEC_WISE (deg)	[pmRA,pmDEC] (mas yr ⁻¹)	pm (mas yr ⁻¹)
09411179+3315130*	145.299135	+33.253632	145.299562	+33.253221	145.300147	+33.252506	[280 (10), -384 (9)]	475
09411195+3315060	145.299803	+33.251675	145.300237	+33.251249	145.300833	+33.250586	[270 (12), -367 (5)]	456
09425716+2351200	145.738183	+23.855574	145.737895	+23.855128	145.737601	+23.854804	[-148 (13), -220 (3)]	266
09430114+2349173	145.754765	+23.821478	145.754459	+23.820927	- ¹	- ¹	[-132 (1), -258 (1)]	290
09425716+2351200	145.738183	+23.855574	145.737895	+23.855128	145.737601	+23.854804	[-148 (13), -220 (3)]	266
09430132+2349222	145.755539	+23.822838	145.755267	+23.822411	145.754933	+23.822075	[-135 (12), -204 (23)]	244
09430114+2349173	145.754765	+23.821478	145.754459	+23.820927	- ¹	- ¹	[-132 (1), -258 (1)]	290
09430132+2349222	145.755539	+23.822838	145.755267	+23.822411	145.754933	+23.822075	[-135 (12), -204 (23)]	244
10294440+2545374	157.435032	+25.760401	157.435232	+25.760251	157.435376	+25.760146	[96 (5), -78 (2)]	124
10294567+2546050	157.440331	+25.768072	157.440522	+25.767925	157.440665	+25.767836	[100 (7), -78 (4)]	127
13034509+2134235*	195.937905	+21.573198	195.937654	+21.573042	195.937332	+21.572885	[-205 (20), -97 (1)]	227
13034574+2134210	195.940608	+21.572527	195.940352	+21.572377	195.940034	+21.572201	[-208 (21), -113 (7)]	237
13090058+1709066	197.252421	+17.151836	197.252184	+17.151897	197.252010	+17.151946	[-94 (10), 46 (7)]	104
13092549+1714584	197.356217	+17.249577	197.355927	+17.249660	197.355776	+17.249696	[-106 (9), 45 (6)]	115
13104398+1434338*	197.683291	+14.576062	197.683245	+14.576131	197.683074	+14.576244	[-81 (8), 66 (2)]	104
13104431+1434326	197.684646	+14.575738	197.684587	+14.575803	197.684390	+14.575869	[-82 (8), 50 (2)]	96
18163409-1246310*	274.142048	-12.775305	274.141560 ²	-12.775722 ²	274.141358	-12.775900	[-199 (11), -194 (10)]	278
18163485-1246421	274.145216	-12.778377	274.144738 ²	-12.778816 ²	274.144515	-12.778945	[-193 (11), -188 (10)]	269

* previously found in WDS catalogue.

¹ Not seen in *WISE*.² GLIMPSE data base coordinates.

- Kaltenegger L., Traub W.A., 2009, *AJ*, 698, 519
- King J. R., Villarreal A. R., Soderblom D. R., Gulliver A. F., Adelman S. J., 2003, *AJ*, 125, 1980
- Knapp G. R. et al., 2004, *AJ*, 127, 3553
- Kouwenhoven M. B. N., Brown A. G. A., Zinnecker H., Kaper L., Portegies Z. S. F., 2005, *A&A* 430, 137
- Kouwenhoven M. B. N., Goodwin S. P., Parker R. J., Davies M. B., Malmberg D., Kroupa P., 2010, *MNRAS*, 404, 1835
- Kouwenhoven M. B. N., Goodwin S. P., Davies M. B., Parker R. J., Kroupa P., Malmberg D., 2011, *ASPC*, 451, 9
- Kraus A. L., Hillenbrand L. A., 2007, *AJ*, 134, 2340
- Kraus A. L., Hillenbrand L. A., 2012, *ApJ*, 757, 141
- Lafrenière D., Jayawardhana R., Janson M., Helling C., Witte S., Hauschildt P., 2011, *ApJ*, 730, 42
- Law N. M., Dhital S., Kraus A., Stassun, K. G., West A. A., 2010, *ApJ*, 720, 1727
- Lawrence A. et al., 2007, *MNRAS*, 379, 1599
- Lépine S., Shara M. M., Rich R. M., 2002, *AJ*, 124, 1190
- Lépine S., Shara M. M., 2005, *AJ*, 129, 1483
- Lépine S., Scholz R. D. 2008, *ApJL*, 681, L33
- Lépine S., Gaidos E., 2011, *AJ*, 142, 138
- Lodieu N., Zapatero-Osorio M. R., Martín E. L., Solano E., Aberasturi M., 2010, *ApJ*, 708, L107
- Lodieu N., Espinoza Contreras M., Zapatero Osorio M. R., Solano Marquez E., Aberasturi M., Martín E. L., 2012, *A&A*, 542A, 105
- López-Morales M., 2007, *ApJ*, 660, 732
- Luhman K. L., 1999, *ApJ*, 525, 466
- Luhman K. L., 2012, *ARA&A*, 50,65
- Luhman K. L., Joergens V., Lada C., Muzerolle J., Pascucci I., White R., 2007, *prpl.conf*, 443
- Luhman K.L., Mamajek E.E., Allen P.R., Muench A.A., Finkbeiner D.P., 2009, *ApJ*, 691, 1265
- Luhman K. L. et al. 2012 *ApJ*, 760, 152
- McElwain M. W., Burgasser A. J., 2006, *AJ*, 132, 2074
- Mclean I. S., McGovern M. R., Burgasser A. J., Kirkpatrick J. D., Prato L., Kim S. S., 2003, *ApJ*, 596, 561
- Mclean I. S., Prato L., McGovern M. R., Burgasser A. J., Kirkpatrick J. D., Rice E., Kim S. S., 2007, *ApJ*, 658, 1217
- Manchado A. et al., 1998, in Fowler A. M., ed., *Proc. SPIE Conf. Vol. 3354, Infrared Astronomical Instrumentation*. SPIE, Bellingham, p. 448
- Mason B.D., Wycoff G.L., Hartkopf W.I., Douglass G.G., Worley C.E., 2001, *AJ*, 122, 3466
- Martín E. L., Delfosse X., Basri G., Goldman B., Forveille T., Zapatero-Osorio M. R., 1999, *AJ*, 118, 2466
- Martín E. L., 2000, *Very Low-mass Stars and Brown Dwarfs*, Edited by R. Rebolo and M. R. Zapatero-Osorio. Published by the Cambridge University Press, UK, 2000., p.119
- Martín E. L., Delfosse X., Guieu S., 2004, *AJ*, 127, 449
- Martín E. L. et al., 2010, *A&A*, 517A, 53
- Mužić K. et al., 2012, *AJ*, 144, 180
- Oke J. B., 1990, *AJ*, 99, 1621O
- Padoan P., Nordlund Å., 2002, *ApJ*, 576, 870
- Pauli E. M., Napiwotzki R., Heber U., Altmann M., Odenkirchen M., 2006, *A&A*, 447, 173
- Radigan J., Lafrenière D., Jayawardhana R., Doyon R., 2009, *ApJ*, 698, 405
- Raghavan D. et al., 2010, *ApJS*, 190, 1
- Rebolo R., Martín E. L., Basri G., Marcy G. W., Zapatero-

Table 3. Physical properties of newly identified low-mass component systems: group A. Components ordered by spectral type, assigning primary position to the earliest type of the componets.

Obj. Id. (2MASS)	Spt. type ¹	T_{eff} ² (K)	$\log g$ ² [cm s^{-2}]	Masses ² (M_{\odot})	Masses ³ (M_{\odot})	Distance (pc)	ρ (arcsec)	Separation (AU)	U (10^{33} J)
00384499+0519003	M4.0	3300	5.5	0.20	0.24	87.53_{-17}^{+14}	549.23	49042	-0.7
00391056+0525351	M6.5	2900	5.0	0.09	0.17	91.05_{-18}^{+15}			
00421418+0431200	M6.5	2900	5.0	0.10	0.17	90.79_{-18}^{+15}	9.03	778	-22.5
00421358+0431185	M7.5	2800	5.0	0.10	0.18	81.43_{-16}^{+13}			
00513688+0735177	M5.0	3000	6.0	0.11	0.20	71.78_{-14}^{+12}	14.72	1110	-17.6
00513590+0735192	M5.5	3000	5.0	0.10	0.18	79.07_{-16}^{+13}			
01463893+1545360	M4.5	3100	4.5	0.11	0.20	53.41_{-11}^{+9}	4.79	257	-93.5
01463861+1545371	M5.0	3100	5.5	0.12	0.18	54.08_{-11}^{+9}			
01560037+0528494	M7.5	2800	5.5	0.09	0.17	77.99_{-15}^{+13}	184.31	13338	-2.4
01554912+0527334	M8.5	2700	4.5	-	0.20	66.74_{-13}^{+11}			
01560053+0528562	M6.0	2900	4.5	0.08	0.17	75.74_{-15}^{+12}	184.31	13338	-2.2
01554912+0527334	M8.5	2700	4.5	-	0.20	66.74_{-13}^{+11}			
01560053+0528562	M6.0	2900	4.5	0.08	0.17	75.74_{-15}^{+12}	7.17	551	-24.1
01560037+0528494	M7.5	2800	5.5	0.09	0.17	77.99_{-15}^{+13}			
01575468+0923422	M5.5	3000	4.5	0.10	0.17	96.77_{-19}^{+16}	10.12	986	-18.4
01575409+0923371	M6.5	2900	4.5	0.10	0.17	98.10_{-19}^{+16}			
02014517+1124244	M2.5	3300	4.5	0.21	0.38	130.66_{-26}^{+22}	586.25	79984	-0.5
02020000+1115202	M5.0	3000	5.0	0.10	0.18	142.20_{-28}^{+23}			
03165635+0617027	M7.0	2800	5.0	0.09	0.18	46.58_{-9}^{+8}	75.91	3525	-3.9
03165886+0618086	M7.0	2800	5.0	0.09	0.18	46.29_{-9}^{+8}			
08255269+2925169	M5.0	3000	5.0	0.10	0.18	98.18_{-19}^{+16}	16.24	1578	-11.9
08255151+2925220	M5.5	3000	5.5	0.11	0.17	96.14_{-19}^{+16}			
09045044-0158572	M3.0	3500	6.0	0.38	0.36	168.64_{-33}^{+28}	34.15	5645	-12.9
09045115-0159297	M6.0	3000	5.0	0.11	0.17	161.99_{-32}^{+27}			
09102559+0648533	M5.0	3100	5.0	0.11	0.19	183.15_{-36}^{+30}	369.64	65247	-0.3
09105025+0648111	M5.5	3000	5.0	0.11	0.17	169.87_{-34}^{+28}			
09335192+3237270	M2.0	3700	6.0	0.51	0.50	160.53_{-32}^{+27}	470.30	81341	-1.0
09332493+3232033	M6.5 (M6 ^a)	2900	5.0	0.09	0.17	185.38_{-37}^{+31}			
09442313+0842231	M4.5	3200	4.5	0.15	0.22	154.59_{-31}^{+26}	7.97	1188	-24.6
09442260+0842235	M6.0	3000	5.5	0.11	0.17	143.81_{-29}^{+24}			
10132950+1135558	M3.5	3100	4.5	0.11	0.27	59.00_{-12}^{+10}	12.92	793	-23.9
10132882+1136041	M6.5	2900	5.5	0.10	0.17	63.67_{-13}^{+10}			
10402749-0248092	M3.5	3400	6.0	0.27	0.30	260.85_{-52}^{+43}	3.59	975	-49.5
10402763-0248063	M5.5	3000	6.0	0.10	0.17	282.76_{-56}^{+47}			
11002544+1445240	M4.5	3100	5.5	0.11	0.20	144.13_{-29}^{+24}	7.58	1161	-19.0
11002578+1445299	M5.0	3100	6.0	0.11	0.19	162.04_{-32}^{+27}			
11242609+1139504	M0.5	4000	6.0	0.70	0.66	181.49_{-36}^{+30}	234.58	4660	-3.0
11243764+1137085	M6.5	3000	6.0	0.11	0.17	215.87_{-43}^{+36}			
12050629+1508193	M3.0	3500	6.0	0.35	0.33	148.61_{-29}^{+25}	454.84	63814	1.0
12043718+1505286	M6.5	2900	6.0	0.10	0.17	131.99_{-26}^{+22}			
12433001-0105152	M3.0	3400	6.0	0.29	0.35	262.19_{-52}^{+43}	18.33	4593	-14.5
12432885-0105208	M5.0	3100	6.0	0.13	0.18	238.91_{-47}^{+40}			

¹ From photometry (Sect. 4.2.4).

² From VOSA (Sect. 4.2.3).

³ From Kraus & Hilenbrand (2007) Table 5 colour-mass relations (Sect. 4.2.3).

^a From spectroscopy. See Sect. 4.3.2.

Table 3. Cont.

Obj. Id. (2MASS)	Spt. type ¹	T_{eff} ² (K)	$\log g$ ² [cm s^{-2}]	Masses ² (M_{\odot})	Masses ³ (M_{\odot})	Distance (pc)	ρ (arcsec)	Separation (AU)	U (10^{33} J)
12593933+0651255	M8.0	2800	4.5	-	0.19	44.56_{-9}^{+7}	23.86	1110	-66.5
12593776+0651204	L0.0	2700	5.0	-	0.21	48.45_{-10}^{+8}			
13002787+2412195	M1.0	3700	6.0	0.60	0.57	171.19_{-34}^{+28}	537.93	91852	-1.5
12594856+2412318	M5.0	3100	5.0	0.13	0.18	170.31_{-34}^{+28}			
13133381+2642533	M4.5	3100	5.0	0.11	0.20	102.31_{-20}^{+17}	5.57	552	-35.2
13133339+2642534	M7.5	2800	5.0	0.10	0.19	95.99_{-19}^{+16}			
13213079+3538516	M3.5	3400	5.5	0.25	0.27	57.13_{-9}^{+11}	4.42	277	-287.8
13213074+3538472	M5.5	3600	6.0	-	0.18	68.21_{-13}^{+11}			
13252369+3555344	M2.5	3500	4.5	0.40	0.43	117.86_{-23}^{+19}	547.79	60450	-0.9
13253949+3604076	M6.5	2800	5.0	0.07	0.17	102.84_{-20}^{+17}			
13261177+3026260	M4.5	3100	5.0	0.11	0.20	226.69_{-45}^{+38}	5.37	1183	-17.2
13261214+3026235	M5.5	3000	5.0	0.10	0.17	213.99_{-42}^{+35}			
13371237+1232212	M3.0	3400	6.0	0.28	0.32	207.56_{-41}^{+34}	361.27	77964	-0.8
13373414+1229314	M5.0	3100	6.0	0.13	0.18	224.05_{-44}^{+37}			
13471881+0746120	M5.5	3000	4.5	0.10	0.17	87.08_{-17}^{+14}	11.49	980	-18.6
13471892+0746006	M6.5	2900	5.5	0.10	0.17	83.37_{-16}^{+14}			
13475983+3343241	M2.5	3400	5.5	0.29	0.37	141.60_{-28}^{+23}	85.60	11523	-4.6
13480028+3341587	M5.5	3000	5.0	0.10	0.17	127.61_{-25}^{+21}			
13490709+1030240	M2.5	3600	6.0	0.45	0.41	212.82_{-42}^{+35}	86.08	19207	-4.6
13490345+1029167	M6.0	3000	5.5	0.11	0.17	233.42_{-44}^{+39}			
13570417+2737490	M4.0	3200	5.0	0.15	0.25	133.59_{-26}^{+22}	125.71	18137	-1.3
13571335+2738194	M6.0	2900	5.0	0.09	0.17	154.95_{-31}^{+26}			
13570929+3403319	M3.5	3300	5.5	0.20	0.28	213.91_{-42}^{+35}	51.04	10084	-3.5
13570535+3403459	M7.0 (M6 ^a)	2900	5.5	0.10	0.17	181.26_{-36}^{+30}			
13572013+0550251	M2.5	3500	5.5	0.39	0.41	164.68_{-33}^{+27}	387.18	67326	-1.1
13565606+0552499	M5.5	3000	5.5	0.11	0.17	183.09_{-36}^{+30}			
16183619+3005336	M6.5	2900	5.5	0.10	0.17	163.62_{-32}^{+27}	428.23	75195	-0.2
16184068+2958293	M7.0	2800	5.5	0.09	0.18	187.56_{-37}^{+31}			
16211986+2653207	M5.0	3000	5.0	0.10	0.18	123.76_{-25}^{+20}	239.57	28622	-0.6
16212591+2649353	M7.5	2800	5.0	0.10	0.19	115.19_{-23}^{+19}			
16234190+3200293	M2.0	3600	4.5	0.50	0.48	166.39_{-33}^{+28}	537.39	83771	-1.1
16241587+3155100	M5.5	3000	6.0	0.11	0.17	145.39_{-29}^{+24}			
22445848+0901564	M3.0	3500	6.0	0.35	0.33	94.35_{-25}^{+11}	314.73	30148	-2.2
22445443+0856474	M5.5	3000	5.5	0.11	0.17	92.09_{-18}^{+15}			
22492577+0516592	M3.5	3500	6.0	-	0.28	52.86_{-13}^{+7}	26.46	1545	-33.3
22492429+0517137	M5.5	3000	5.0	0.10	0.18	61.52_{-12}^{+10}			
23253026+1434102	M6.5	2900	5.5	0.09	0.17	133.00_{-20}^{+16}	9.77	1220	-27.6
23253016+1434198	M9.0	2700	5.0	-	0.21	122.13_{-24}^{+20}			
23283688+0822011	M5.0	3000	5.0	0.10	0.18	97.24_{-19}^{+16}	480.24	48540	-0.7
23280466+0821168	M8.0	2800	5.5	-	0.20	104.96_{-21}^{+17}			
23433880+1304223	M3.5	3300	5.5	0.20	0.27	106.39_{-21}^{+18}	548.07	58713	-1.2
23435793+1256309	M8.0	2800	5.5	-	0.19	107.67_{-22}^{+18}			

¹ From photometry (Sect. 4.2.4).² From VOSA (Sect. 4.2.3).³ From Kraus & Hilenbrand (2007) Table 5 colour-mass relations (Sect. 4.2.3).^a From spectroscopy. See Sect. 4.3.2.

Table 4. Physical properties of newly identified low-mass component systems: group B. Components ordered by spectral type, assigning primary position to the earliest type of the componets.

Obj. Id. (2MASS)	Spt. type ¹	T_{eff} ² (K)	$\log g$ ² [cm s ⁻²]	Masses ² (M_{\odot})	Masses ³ (M_{\odot})	Distance (pc)	ρ (arcsec)	Separation (AU)	U (10 ³³ J)
09411195+3315060	M5.0	3500 ^a	4.5	-	0.18	30.10 ^b	7.44	244	-299.5
09411179+3315130	L0.0	2500	4.5	-	0.23	35.52			
09430132+2349222	M0.5	3800	6.0	-	0.46	31.55	133.39	4640	-35.0
09425716+2351200	M8.5 (M7 ^c)	2700	4.5	-	0.20	34.12			
09430114+2349173	M7.0	2700	5.5	0.06	0.14 ^d	38.68 ^e	134.10	4715	-10.0
09425716+2351200	M8.5 (M7 ^c)	2700	4.5	-	0.20	34.12			
09430132+2349222	M0.5	3800	6.0	-	0.46	31.55	5.6	195	-249.8
09430114+2349173	M7.0	2700	5.5	0.06	0.14 ^d	38.68 ^e			
10294440+2545374	M4.0	3200	4.5	0.15	0.18	26.77	33.56	950	-19.5
10294567+2546050	M6.5	2800	4.5	0.07	0.17	29.82			
13034509+2134235	M6.0	2900	4.5	0.11	0.17	61.59	10.03	605	-28.9
13034574+2134210	M8.0	2700	5.5	0.09	0.19	58.99			
13092549+1714584	M6.5 (M6 ^c)	2800	5.0	0.07	0.17	74.39	513.26	39878	-0.22
13090058+1709066	M7.5 (M7 ^c)	2800	5.5	0.07	0.18	81.00			
13104431+1434326	M7.0	2800	4.5	-	0.17	65.68	5.01	333	-162.2
13104398+1434338	M7.5	2800	4.5	-	0.18	67.32			
18163409-1246310	M2.0 ^f (M4-M6 ^c)	3500	5.0	-	0.45 ^g	42.27 ^h	15.85	698	-182.1
18163485-1246421	M4.5 ^f (M5-M6 ^c)	3100	5.5	-	0.16 ^g	45.79 ^h			

¹ From photometry (Sect. 4.2.4).

² From VOSA (Sect. 4.2.3).

³ From Kraus & Hilenbrand (2007) Table 5 colour-mass relations (Sect. 4.2.3).

^a No good fit of the SED was found, 3500-3600 K was the best but we take his value with caution, relying more in the temperature obtained by other methods.

^b From $M_r - (i - z)$ relation in Bochanski et al. (2010; Table 4), since the (r-z) colour is outside the allowed range for the $M_r - (r - z)$ calibration. See Sect. 4.2.1.

^c From spectroscopy. See Sect. 4.3.2.

^d From M_i and M_r since z value is not reliable.

^e From $M_r - (r - i)$ relation in Bochanski et al. (2010; Table 4), since z value is not reliable. See Sect. 4.2.1.

^f From $(H - K_s)$ colour (Sect. 4.2.4).

^g From M_J relations in Kraus & Hilenbrand (2007). See Sect. 4.2.3.

^h From M_J -spectral type relation in Hawley et al. (2002) (Sect. 4.2.4).

Table 5. Physical properties of the identified higher mass tertiaries to the M-M systems

System Id. (2MASS)	PPMXL ID.	RA (deg)	DEC (deg)	[pmRA, pmDEC] (mas yr ⁻¹)	Spt. Type	T_{eff} (K)	Masses M_{\odot}	Distance (pc)	Separation (AU)	U (10 ³³ J)
02014517+1124244 02020000+1115202	2102675187759530038	29.854309	11.281106	[65 (1.6),-32 (1.6)]	G7	5500	0.90	148.08	275725.81	1.8
09335192+3237270 09332493+3232033	4233992647964279227	143.245865	32.478501	[-61 (4.8),-38 (4.8)]	K6	4400	0.64	163.30	136476.81	5.0
09335192+3237270 09332493+3232033	4234014784472339948	143.566876	32.607488	[-51 (2.0),-49 (2.1)]	K0	5200	0.80	189.97	49867.50	17.0
11242609+1139504 11243764+1137085	4137926243272078734	171.108659	11.664022	[75 (5.3),-72 (5.3)]	K7	4300	0.61	156.89	50676.59	17.2
13475983+3343241 13480028+3341587	4551655942546822025	207.003151	33.742283	[78 (3.8),-135 (3.8)]	K9	3900	0.60	141.65	9775.82	42.2
13572013+0550251 13565606+0552499	4398878071445995714	209.242262	5.856395	[-37 (4.6),-40 (4.6)]	K0	5200	0.80	164.47	54876.92	12.9

Table 6. Physical properties of the new L-F system

Obj. Id.	[pmRA,pmDEC]/pm (mas yr ⁻¹)	Spt. type	T_{eff}^1 (K)	$\log g^1$ [cm s ⁻²]	Masses (M_{\odot})	Distance (pc)	Separation (AU)	U (10 ³³ J)
2MASS 09320299+1231027	[-125 (7.1), -113 (7.1)]/169	L2.0 ^a	2300.0	5.5	0.075 ^b	40	130450	1.2
PPMXL 4077732287929300487	[-111 (1.0), -125 (0.6)]/167	F8.0 ^c	6100.0		1.19 ^c	52		

¹ From VOSA (Sect. 4.2.3).^a From photometry (Sect. 4.2.4).^b Value state by default for an L dwarf. See Sect 6.^c From temperature and spectral types in Gray (1992). See Sect 6.

Osorio M. R., 1996, ApJ, 469L, 53
 Reid I. N., Gizis J. E., 1997, AJ, 114, 1992
 Reid I. N., Gizis J. E., Kirkpatrick J. D., Koerner D. W., 2001, AJ, 121, 489
 Reid I. N., Cruz K. L., Allen P. R., 2007, AJ, 133, 2825
 Reid I. N., Hawley S. L., 2005, New light on dark stars : red dwarfs, low-mass stars, brown dwarfs. Praxis Publishing Ltd, Chichester, UK
 Reid I. N., Walkowicz L. M., 2006, PASP, 118, 671
 Reipurth B., Clarke C., 2001, AJ, 122, 432
 Roeser S., Demleitner M., Schilbach E., 2010, AJ, 139, 2440
 Salim S., Gould A., 2002, ApJL, 575, L83
 Schlieder J. E., Lépine S., Rice E., Simon M., Fielding D., Tomasino R., 2012, AJ, 143, 114S
 Schmidt S. J., West A. A., Hawley S. L., Pineda S., 2010, AJ, 139, 1808
 Seifahrt A., Guenther E., Neuhiäuser R., 2005, A&A, 440, 967
 Shkolnik E., Liu M. C., Reid I. N., 2009, ApJ, 699, 649
 Siegler N., Close L. M., Cruz K. L., Mart'in E.L., Reid I. N., 2005, AJ, 621, 1023
 Skrutskie M. F. et al., 2006, AJ, 131, 1163
 Stelzer B., Marino A., Micela G., López-Santiago J., Liefke, 2013, MNRAS, 431, 2063
 Tody D., 1986, in Society of Photo-Optical Instrumentation Engineers (SPIE) Conference Series, Vol. 627, Society of Photo-Optical Instrumentation Engineers (SPIE) Conference Series, ed. D. L. Crawford, 733
 Tody D., 1993, in Astronomical Society of the Pacific Conference Series, Vol. 52, Astronomical Data Analysis Software and Systems II, ed. R. J. Hanisch, R. J. V. Brissenden, & J. Barnes, 173
 Tokovinin A., Lpine, S., 2012, AJ, 144, 102
 van Leeuwen, F. 2007, A&A, 474, 653
 Valdivielso L., et al., 2009, A&A, 497, 973
 Weinberg M. D., Shapiro S. L., Wasserman I., 1987, ApJ, 312, 367
 West A. A., Hawley S. L., Bochanski J. J., Covey K. R., Reid I. N., Dhital S., Hilton E. J., Masuda M., 2008, The Astronomical Journal, 135, 785
 West A. A. et al., 2011, AJ, 141, 97
 Whitworth A. P., Bate M. R., Nordlund Å., Reipurth B., Zinnecker H., 2007, prpl.conf,459
 Whitworth A. P., Zinnecker H., 2004, A&A, 427, 299
 Wilson J. C., Kirkpatrick J. D., Gizis J. E., Skrutskie M. F., Monet D. G., Houck J. R., 2001, AJ, 122, 1989
 Wright E. L., et al., 2010, AJ, 140, 1868
 Zacharias N., Finch C. T., Girard T. M., Henden A.,

Bartlett J. L., Monet D. G., Zacharias M. I., 2013, AJ, 145, 44Z
 Zhang et al., 2017, MNRAS, 464, 3040
 Zhao J. K., Oswalt T. D., Rudkin M., Zhao G., Chen Y. Q., 2011, AJ, 141, 107

This paper has been typeset from a \LaTeX file prepared by the author.

APPENDIX A: TABLES

Table A1. L-T Candidates.

2MASS	RA_2MASS (deg)	DEC_2MASS (deg)	RA_SDSS (deg)	DEC_SDSS (deg)	2MASS-J (2MASS)	[pmRA,pmDEC] (mas yr ⁻¹)	pm (mas yr ⁻¹)	Spt. type ¹	T _{eff} ² (K)	logg ² [cm s ⁻²]	Dist. (pc)
00062250+1300451	1.593781	13.012551	1.593775	13.012333	16.96	[-2, -69]	69	L2.0	1800	5.5	78
00081285+0806441	2.053555	8.11226	2.053566	8.111889	16.59	[8, -270]	270	L1.5	2000	4.5	70
00363231+0722108	9.134658	7.369681	9.134572	7.369572	16.55	[-61, -78]	99	L1.5	2500	4.5	72
01250319+0840499	21.263297	8.680554	21.263427	8.680479	16.47	[57, -33]	66	L2.0	1600	4.5	57
02151451+0453179	33.810475	4.888312	33.810537	4.887977	16.60	[27, -148]	151	L2.5	1500	5.0	65
03074939+0516533	46.955794	5.281497	46.955758	5.28135	16.64	[-30, -123]	127	L2.5	1500	5.0	57
07415323+2129056	115.471829	21.484909	115.471803	21.485079	16.64	[-18, 124]	125	L2.5	2300	4.5	75
08064841+2215456	121.701749	22.262667	121.701728	22.262519	16.99	[-22, -171]	172	L1.0 ^a	1700	4.5	94 ^a
08223262+0442042	125.64844	4.701173	125.648228	4.701246	16.75	[-372, 128]	393	L5.0	1800	5.0	33
08330964+2949094	128.290178	29.819294	128.29016	29.819006	16.34	[-11, -211]	211	L2.5	1600	5.0	49
08532128-0117039	133.33867	-1.284424	133.338385	-1.284338	16.69	[-125, 38]	130	L2.0	2400	4.5	68
09165461+0546086	139.227582	5.769081	139.227618	5.768987	16.24	[63, -166]	178	L2.0	1500	5.5	53
09320299+1231027	143.012464	12.517433	143.012209	12.517207	15.60	[-125, -113]	169	L2.0	2300	5.5	40
09412866+0504166	145.369443	5.071281	145.36924	5.071271	16.37	[-102, -5]	102	L1.5	2500	4.5	59
09443669+3356113	146.152891	33.936493	146.152801	33.936618	16.87	[-45, 76]	88	L2.5	2400	4.5	61
09461127+3027152	146.546992	30.454231	146.546882	30.454104	16.74	[-57, -76]	95	L2.0	2400	4.5	76
10355745+1149420	158.98938	11.828347	158.989305	11.828318	16.12	[-95, -37]	102	L1.5 ^b	2200	5.5	57
10505470-0048352	162.727918	-0.809791	162.727382	-0.809848	16.17	[-234, -25]	235	L1.5 ^b	2500	5.0	59
10520456+0617307	163.019035	6.291863	163.018792	6.291908	16.87	[-445, 83]	452	L3.5	2000	5.5	55
10580444+1339474**	164.518513	13.663172	164.517942	13.663039	16.43	[-332, -79]	341	L2.5	2400	5.5	49
11025112+1040469	165.713021	10.679718	165.712878	10.679678	16.34	[-166, -47]	172	L2.5	2500	4.5	57
11072127+1754418	166.838629	17.911617	166.838517	17.911491	16.76	[-52, -61]	80	L1.5	1800	5.5	72
11082937+1543012	167.122404	15.717017	167.122135	15.717025	16.69	[-125, 4]	125	To-T2 ^c	1800	5.0	- ^c
11220855+0343193	170.535636	3.722044	170.535561	3.722026	15.65	[-231, -56]	238	L3.0	2300	4.5	38
11243866+1542585	171.161099	15.716263	171.160612	15.716392	16.70	[-283, 78]	293	L2.0	2500	5.5	68
11305248+1638019**	172.718694	16.633886	172.718339	16.633741	16.46	[-199, -85]	216	L1.5	2500	5.0	70
11411784+0108184	175.324349	1.138468	175.324255	1.138331	16.27	—	—	L2.0	2400	5.5	56
12051260+1245381	181.30254	12.760606	181.302397	12.760703	16.39	[-96, 67]	117	L2.0	2400	4.5	56
12594167+1001380	194.923656	10.027239	194.923584	10.027265	16.82	[-130, 48]	138	L4.0	1700	5.0	54
13023109+2648294	195.629559	26.808191	195.629383	26.808316	16.79	[-99, 79]	127	L2.5	1800	5.5	62
13084263+0432441*	197.177664	4.54559	197.177768	4.545449	16.07	[341, -463]	575	L1.5	2500	5.0	56
13211687+2755329	200.320319	27.925825	200.320568	27.925768	16.81	[157, -41]	162	L1.5	2200	5.5	89
13284086+0746280	202.170254	7.774453	202.169892	7.774319	16.10	[-209, -78]	223	L2.0	2400	4.5	51
13364870+2134050	204.20292	21.568056	204.202661	21.568029	16.88	[-147, -16]	148	L2.5	2200	5.5	67
13493145+2945533	207.38108	29.764826	207.381004	29.764848	15.77	[-58, 19]	061	L2.0	1800.0	5.5	43
13510003+2925273	207.750126	29.424257	207.749752	29.424225	16.97	[-291, -28]	292	To-T2 ^c	1200	4.5	- ^c
14025073+3639378	210.711385	36.660507	210.711031	36.660493	16.98	[-204, -10]	204	L2.5	2000	5.5	43
14092137+0818363	212.339044	8.310092	212.339011	8.309978	16.09	[-38, -133]	139	L1.5	1800	5.0	90
14120397+1216100	213.016546	12.269448	213.016283	12.269446	16.39	[-268, -2]	268	L4.0	1900	4.5	34
14193426+1413257	214.892778	14.223807	214.892742	14.223641	16.54	[-20, -95]	97	L1.5	2400	4.5	70
14313545-0313117	217.897746	-3.219942	217.897317	-3.219785	16.09	[-189, 69]	202	L5.0	1800	5.0	23
15210289-0008348	230.262079	-0.143	230.262281	-0.143074	16.66	—	—	L2.0	1800	4.5	70
15543602+2724487	238.650105	27.413544	238.650176	27.413418	16.19	[72, -145]	162	L4.0	1800	5.5	31
20595810-0012356	314.992101	-0.209907	314.992026	-0.210154	16.74	[-53, -175]	183	L2.5	1800	5.0	68
22195949+0451337	334.997876	4.859363	334.998038	4.859271	16.35	[70, -40]	81	L2.0	2400	5.5	59
22355244+0418563	338.968505	4.31564	338.967821	4.315269	15.37	[-301, -163]	342	L4.5	1800	5.5	20
22525796+0209332	343.241504	2.159227	343.241795	2.158899	16.61	[129, -145]	194	L1.5	2200	4.5	69
23004298+0200145	345.179123	2.004042	345.179428	2.004025	16.40	[136, -8]	136	L3.5	1700	4.5	53
23132142+0253472	348.339288	2.896458	348.338946	2.896158	16.80	[-152, -133]	202	L2.0	2300	5.0	67
23292520+1009302	352.355018	10.158415	352.354921	10.158206	16.45	[-42, -93]	102	L2.0	2300	4.5	56

¹ From photometry (Sect. 4.2.4).² From VOSA (Sect. 4.2.3).^a From ($i - J$) colour-spectral type relation of Schmidt et al. (2010) only since ($i - z$) criterion is not fulfilled.^b Classified as L dwarf by SDSS pipeline.^c Since ($i - z$) and ($i - J$) criteria of Schmidt et al. (2010) are not fulfilled, the spectral type is calculated from the rest of the colours in Table 3 of Schmidt et al. (2010).

* These objects may correspond to low metallicity Ls, or L subdwarfs, due to their proper motion and colours characteristics, see Sect. 5.

** Spectrum of the target is available and discussed in Sect. 5.

Table A2. Wide low mass Binaries from the literature. Separations over 200 AU and total system masses under 1 M_{\odot} .

Name ¹	Separation (AU)	Masses P (M_{\odot})	Masses S ² (M_{\odot})	U (10^{33} J)	References
2M1043+1706 AB	1020	0.21	0.08	-29	Baron et al. (2015)
LSPM J1021+3704 & 2M1021+3704	3000	0.21	0.07	-8.6	Baron et al. (2015)
LSPM J1236+3000 & 2M1236+3000	1580	0.10	0.08	-8.9	Baron et al. (2015)
LSPM J1259+1001 & 2M1259+1001	345	0.12	0.06	-36.7	Baron et al. (2015)
LSPM J1441+1856 & 2M1441+1856	4110	0.10	0.07	-3.0	Baron et al. (2015)
NLTT 182 & 2M0005+0626	400	0.16	0.08	-56.3	Baron et al. (2015)
NLTT 251 & 2M0006-0852	850	0.10	0.08	-16.6	Baron et al. (2015)
NLTT 687 & 2M0013-1816	7400	0.39	0.07	-6.5	Baron et al. (2015)
NLTT 2274 & 2M0041+1341	725	0.21	0.08	-40.8	Baron et al. (2015)
NLTT 20640 & 2M0858+2710	780	0.21	0.07	-33.1	Baron et al. (2015)
NLTT 26746 & 2M1115+1607	660	0.21	0.06	-33.6	Baron et al. (2015)
NLTT 29392 & 2M1202+4204	1310	0.10	0.07	-39.7	Baron et al. (2015)
NLTT 30510 & 2M1222+3643	660	0.38	0.07	-28.6	Baron et al. (2015)
NLTT 36369 & 2M1408+3708	590	0.21	0.09	-56.4	Baron et al. (2015)
HIP 49046 AB	4720	0.60	0.09	-20.1	Deacon et al. (2014)
HIP 60501 AB	2100	0.60	0.14	-70.4	Deacon et al. (2014)
HIP 63506 AB	5640	0.60	0.06	-11.2	Deacon et al. (2014)
HIP 73169 AB	796	0.60	L2.5	-	Deacon et al. (2014)
HIP 78184 AB	3829	0.60	0.075	-20.6	Deacon et al. (2014)
LSPM J1336+2541 AB	8793	0.36	L4	-	Deacon et al. (2014)
LSPM J2153+1157 AB	408	0.36	0.09	-139.8	Deacon et al. (2014)
NLTT 730 AB	5070	0.20	L7.5	-	Deacon et al. (2014)
NLTT 8245 AB	562	0.60	0.09	-169.1	Deacon et al. (2014)
NLTT 18587 AB	12200	0.44	0.08	-5.1	Deacon et al. (2014)
NLTT 19109 AB	362	0.20	0.08	-77.8	Deacon et al. (2014)
NLTT 22073 AB	776	0.44	0.08	-79.8	Deacon et al. (2014)
NLTT 26746 AB	661	0.20	L4	-	Deacon et al. (2014)
NLTT 27966 AB	630	0.14	L4	-	Deacon et al. (2014)
NLTT 29395 AB	671	0.36	0.08	-75.5	Deacon et al. (2014)
NLTT 30510 AB	962	0.44	0.07	-56.3	Deacon et al. (2014)
NLTT 31450 AB	487	0.20	L6	-	Deacon et al. (2014)
NLTT 38489 AB	418	0.20	0.075	-63.1	Deacon et al. (2014)
NLTT 39312 AB	713	0.44	0.08	-86.9	Deacon et al. (2014)
NLTT 44368 AB	7760	0.36	L1.5	-	Deacon et al. (2014)
NLTT 52268 AB	549	0.36	0.075	-86.6	Deacon et al. (2014)
NLTT 55219 AB	432	0.44	L5.5	-	Deacon et al. (2014)
PMI 13410+0542 AB	484	0.49	L4	-	Deacon et al. (2014)
PMI 13518+4157 AB	613	0.40	L1.5	-	Deacon et al. (2014)
PMI 221181005 AB	8892	0.44	L1.5	-	Deacon et al. (2014)
PMI 23492+3458 AB	949	0.44	L9	-	Deacon et al. (2014)
LHS 6176 & ULAS J095047.28+011734.3	1400	0.28	T8	-	Luhman et al. (2012)
G259-20 & 2MASS J17430860+8526594	650	0.40	L5	-	Høg et al. (2000), Luhman et al. (2012)
LHS 3421 & 2MASS J18525777570814	1500	0.40	-	-	van Leeuwen (2007), Hawley et al. (1996), Luhman et al. (2012)
LSPM J2010+0632 & 2MASS J20103539+0634367	2100	0.28	0.08	-18.7	Luhman et al. (2012)
2MASS J05254550-7425263 & 2MASS J05253876-7426008	2020	0.46	0.07	-28.1	Mužić et al. (2012)
2MASS J13480721-1344321 & 2MASS J13480290-1344071	1400	0.18	0.04	-9.1	Mužić et al. (2012)
NLTT 2274 & SDSS J004154.54+134135.5	483	0.20	0.06	-43.7	Faherty et al. (2010)
G73-26 & SDSS J020735.60+135556.3	2774	0.44	L2	-	Faherty et al. (2010)
G121-42 & 2MASS J12003292+2048513	5916	0.20	0.09	-5.3	Faherty et al. (2010)
G204-39 & SDSS J175805.46+463311.9	2685	0.36	0.02	-4.8	Faherty et al. (2010)
LP 213-67 ^a	230	0.10	0.18	-138.1	Gizis et al. (2000), Close et al. (2003), Faherty et al. (2010)
Wolf 940 & ULAS 2146	400	0.20	0.03	-26.5	Burningham et al. (2009), Faherty et al. (2010)
LP 261-75 & 2MASS J09510549+3558021	450	0.22	0.02	-17.2	Reid & Walkowicz (2006), Faherty et al. (2010)
G1 618.1 AB	1090	0.67	0.06	-65.1	Wilson et al. (2001), Faherty et al. (2010)
G124-62 & DENIS-P J1441-0945	1496	0.21	0.07	-17.3	Seifahrt et al. (2005), Faherty et al. (2010)
2MASS J12583501+4013083 & 2MASS J12583798+4014017	6700	0.11	0.09	-26.1	Radigan et al. (2009), Faherty et al. (2010)
FU Tau AB	800	0.05	0.015	-1.6	Luhman et al. (2009)
2M012650 AB	5100	0.095	0.092	3.0	Caballero (2009), Artigau et al. (2007)
2M1258+40 AB	6700	0.105	0.091	2.5	Caballero (2009), Radigan et al. (2009)
AU Mic & AT Mic AB	46400	0.45	0.52	-7.7	Caballero (2009)
LEHPM 494 & DE 002142 (K1 AB)	1800	0.103	0.079	8.0	Caballero (2007a,b) & (2009)
LP 655-23 & 2M 0430-08 (K2 AB)	450	0.26	0.086	-87.7	Caballero (2007b)
SE70 & S Ori68	1700	0.045	0.005	-0.2	Caballero et al. (2006)
DENIS J055146.0-443412.2 AB	220	0.085	0.079	-53.5	Burgasser et al. (2007)
2MASS J11011926-7732383 AB	242	0.05	0.025	-9.1	Siegler et al. (2005), Burgasser et al. (2007)
Gliese 150.1 AB	2400	0.57	0.46	-191.7	Fischer & Marcy (1992)
Gliese 277 AB	550	0.39	0.27	-335.9	Fischer & Marcy (1992)
Gliese 589 AB	240	0.25	0.11	-201.0	Fischer & Marcy (1992)
Gliese 644 AC	1730	0.33	0.09	-30.1	Fischer & Marcy (1992)
Gliese 669 AB	210	0.30	0.20	-501.3	Fischer & Marcy (1992)
Gliese 720 AB	2075	0.53	0.22	-98.6	Fischer & Marcy (1992)
Gliese 745 AB	1300	0.27	0.27	-98.4	Fischer & Marcy (1992)
Gliese 752 AB	545	0.42	0.08	-108.2	Fischer & Marcy (1992)

¹ As appeared in reference paper.² For spectral types later than L0 without mass determination in the literature, no mass has been assigned.^a B component is a binary M8+L0. Its total mass is larger than primary M6.4 mass.

Table A3. Wide low mass Binaries from the literature (cont.): SLoWPoKES I.

Name SLoWPoKES	Separation (AU)	Total Mass ¹ (M _⊙)	U ¹ (10 ³³ J)
SLW0020-15	1324	0.69	-329.3
SLW0250+19	26411	0.35	-2.7
SLW1521+26	15772	0.39	-6.5
SLW1540+13	13983	0.35	-4.5
SLW0721+35	2714	0.35	-22.3
SLW0903+06	7330	0.35	-7.9
SLW0935+51	3564	0.75	-124.4
SLW1204+19	994	0.30	-32.9
SLW0236-01	16955	0.34	-43.9
SLW0903+53	3326	0.43	-44.9
SLW1318+47	3031	0.39	-28.8
SLW1410+01	1299	0.50	-171.9
SLW1542+50	6125	0.29	-4.3
SLW1027+49	1960	0.31	-22.9
SLW1116+05	2618	0.42	-45.5
SLW1146+43	1589	0.43	-99.9
SLW1259+47	902	0.39	-94.5
SLW1121+58	1362	0.32	-50.4
SLW0336-05	440	0.30	-93.3
SLW1417+13	1211	0.39	-68.7
SLW1242+24	1561	0.30	-23.6
SLW0820+56	510	0.39	-268.2
SLW0105+15	538	0.31	-107.6
SLW1259+19	1975	0.24	-10.5
SLW1840+42	870	0.21	-22.8

¹ Binding energies are calculated using estimated masses as a function of spectral type (Kraus & Hillenbrand 2007). When spectral type not available, it was assumed to be an equal-mass binary, Dhital et al. (2010).